# The nitrogen budget of laboratory-simulated western U.S. wildfires during the FIREX 2016 FireLab study

James M. Roberts[1], Chelsea E. Stockwell[1,2@], Robert J. Yokelson[3], Joost de Gouw[1,2,5], Yong Liu[4], Vanessa Selimovic[3], Abigail R. Koss[1,2,5*], Kanako Sekimoto[1,2,6], Matthew M. Coggon[1,2], Bin Yuan[1,2,†], Kyle J. Zarzana[1,2,Δ], Steven S. Brown[1], Cristina Santin[7], Stefan H. Doerr[7], and Carsten Warneke[1,2]

[1]NOAA Earth System Research Laboratories (ESRL), Chemical Sciences Laboratory, Boulder, CO, USA.
[2]Cooperative Institute for Research in Environmental Sciences, University of Colorado Boulder, Boulder, CO, USA.
[3]Department of Chemistry and Biochemistry, University of Montana, Missoula, MT, USA.
[4]Department of Chemistry, University of Colorado, Denver, Denver, Colorado, USA.
[5]Department of Chemistry, University of Colorado Boulder, Boulder, CO, USA.
[6]Graduate School of Nanobioscience, Yokohama City University, Yokohama, Japan.
[7]Departments of Geography and Biosciences, Swansea University, Swansea, UK.
* now at Tofwerk, USA, Boulder, CO, USA.
† now at Institute for Environmental and Climate Research, Jinan University, Guangzhou, China.
@ now at Scientific Aviation, Boulder, CO., USA.
Δ now at Department of Chemistry, University of Colorado Boulder, Boulder, CO, USA.

*Correspondence to:* James M. Roberts (james.m.roberts@noaa.gov)

**Abstract.** Reactive nitrogen ($N_r$, defined as all nitrogen-containing compounds except for $N_2$ and $N_2O$) is one of the most important classes of compounds emitted from wildfire, as $N_r$ impacts both atmospheric oxidation processes and particle formation chemistry. In addition, several $N_r$ compounds can contribute to health impacts from wildfires. Understanding the impacts of wildfire on the atmosphere requires a thorough description of $N_r$ emissions. Total reactive nitrogen was measured by catalytic conversion to NO and detection by NO-$O_3$ chemiluminescence together with individual $N_r$ species during a series of laboratory fires of fuels characteristic of Western U.S. wildfires, conducted as part of the FIREX FireLab 2016 study. Data from 75 stack fires were analyzed to examine the systematics of nitrogen emissions. The measured $N_r$/total-carbon ratios averaged 0.37% for fuels characteristic of western North America and these gas phase emissions were compared with fuel and residue N/C ratios and mass to estimate that a mean (±std. dev.) of 0.68 (±0.14) of fuel nitrogen was emitted as $N_2$ and $N_2O$. The $N_r$ detected as speciated individual compounds included: nitric oxide (NO), nitrogen dioxide ($NO_2$), nitrous acid (HONO), isocyanic acid (HNCO), hydrogen cyanide (HCN), ammonia ($NH_3$), and 44 nitrogen-containing volatile organic compounds (NVOCs). The sum of these measured individual $N_r$ compounds averaged 84.8 (±9.8)% relative to the total $N_r$, and much of the 15.2% "unaccounted" $N_r$ is expected to be particle-bound species, not included in this analysis.

A number of key species, e.g. HNCO, HCN and HONO, were confirmed not to correlate only with flaming or only with smoldering combustion when using modified combustion efficiency (MCE = $CO_2$/(CO + $CO_2$)) as a rough indicator. However, the systematic variations of the abundance of these species relative to other nitrogen-containing species were successfully modeled using positive matrix factorization (PMF). Three distinct factors were found for the emissions from combined coniferous fuels: a combustion factor (Comb-N) (800-1200°C) with emissions of the inorganic compounds NO, $NO_2$ and HONO, and a minor contribution from organic nitro compounds (R-$NO_2$); a high-temperature pyrolysis factor (HT-N) (500-800°C) with emissions of HNCO, HCN and nitriles; and a low-

temperature pyrolysis factor (LT-N) (<500°C) with mostly ammonia, and NVOCs. The temperature ranges specified are based on known combustion and pyrolysis chemistry considerations. The mix of emissions in the PMF factors from chaparral fuels (manzanita and chamise) had a slightly different composition: the Comb-N factor was also mostly NO, with small amounts of HNCO, HONO and $NH_3$, the HT-N factor was dominated by $NO_2$ and had HONO, HCN, and HNCO, and the LT-N factor was mostly $NH_3$ with a slight amount of NO contributing. In both cases, the Comb-N factor correlated best with $CO_2$ emission, while the HT-N factors from coniferous fuels correlated closely with the high temperature VOC factors recently reported by Sekimoto et al., (2018) and the LT-N had some correspondence to the LT-VOC factors. As a consequence, $CO_2$ is recommended as a marker for combustion $N_r$ emissions, HCN is recommended as a marker for HT-N emissions and the family $NH_3$/particle ammonium is recommended as a marker for LT-N emissions.

## 1 Introduction

Wildfires have severe impacts on the chemistry of the atmosphere from local to global scales (Crutzen and Andreae, 1990). A warmer, drier climate in western North America, coupled with policies that have allowed build-up of fuels in forest ecosystems has led to increases in frequency and severity of wildfires in this region (Abatzoglou and Williams, 2016; Westerling et al., 2006). The new strategy for management of wildfire in the U.S. is to allow fire where possible and to fight fire where needed (Lee et al., 2014). The science behind making these decisions and understanding their consequences involves, in part, a better understanding of the emissions from wildfires. The NOAA FIREX (Fire Influence on Regional and Global Environments Experiment) FireLab experiment was conducted in the Fall of 2016, at the U.S. Forest Service Fire Sciences Laboratory in Missoula, Montana, to acquire detailed measurements of particle and gas-phase emissions from fires involving fuels characteristic of the western U.S. (NOAA, 2018). Several aspects of these measurements dealing with VOC species, and individual reactive nitrogen species ($N_r$, defined as all nitrogen compounds except for $N_2$ and $N_2O$) have already been published (Koss et al., 2018; Manfred et al., 2018; Sekimoto et al., 2018; Selimovic et al., 2018; Zarzana et al., 2018), including emissions factors for many of the $N_r$-species (Koss et al., 2018).

The $N_r$ compounds emitted by natural-convection biomass burning (BB) arise solely from the N in the fuels, since the combustion temperatures are not high enough (<1200°C) to produce oxides of nitrogen (NOx) from $N_2$ and $O_2$ (the so-called Zeldovich or thermal nitrogen cycle) (Lobert and Warnatz, 1993; Taylor et al., 2004; Wotton et al., 2012). The fuel nitrogen cycles that pertain to BB flaming combustion are shown schematically in Figure 1 (Glarborg et al., 2018; Lobert and Warnatz, 1993; Lucassen et al., 2012; Manion et al., 2015). Note that the equations shown in Figure 1 are meant to indicate the general flow of the chemistry and do not always convey the mechanistic subtleties of the reactions, which are fully covered in specialized references (Glarborg et al., 2018; Manion et al., 2015). $N_r$ compounds are emitted as small molecules, hydrogen cyanide (HCN), isocyanic acid (HNCO), and ammonia ($NH_3$) resulting from pyrolysis of the fuel, with minor contributions from larger N-containing organic species, especially at lower temperatures. Flame chemistry converts those species to $N_2$, $N_2O$, nitric oxide (NO), nitrogen dioxide ($NO_2$), and nitrous acid (HONO) as a result of radical chemistry. It has been recognized for some time that a significant amount of denitrification (conversion of $N_r$ compounds to $N_2$) occurs due to reactions of NO with $NH_i$ (where i= 1, 2,

or 3) or N atoms, as confirmed experimentally (Kuhlbusch et al., 1991). While N atoms are also intermediates in the thermal $NO_x$ cycle and the reaction $N + O_2 \rightarrow NO + O$ figures in to both the fuel and thermal $NO_x$ cycles, the second reaction of the thermal $NO_x$ cycle, $O + N_2 \rightarrow NO + N$, is too slow at BB flame temperatures to result in $NO_x$ production (Manion et al., 2015). In addition to the small molecules shown in Figure 1, numerous $N_r$-compounds are emitted in roughly the following categories: amides, amines, heterocyclic compounds, nitriles, isocyanates, and nitro compounds (Andreae, 2019; Andreae and Merlet, 2001; Koss et al., 2018; Lobert et al., 1991; Lobert et al., 1990; Lobert and Warnatz, 1993; Stockwell et al., 2015). These compounds are produced at much lower abundance from fuel pyrolysis and partial reactions with the radical species in Figure 1.

The emissions of N-compounds from BB and wildfires in general have been the subject of considerable research. Early studies by Lobert et al., (1990, 1991, 1993) measured a wide range of $N_r$ compounds in laboratory fires and suggested that considerable denitrification (conversion of fuel nitrogen to $N_2$) was taking place, a process later confirmed in experiments described by Kuhlbusch et al., (1991). Subsequent work on laboratory fires has better defined particle phase nitrogen emissions (McMeeking et al., 2009) and led to the recognition of the importance of several inorganic $N_r$ species, such as HONO and HNCO (Burling et al., 2010; Roberts et al., 2011; Veres et al., 2010), and the presence of a wider variety of organic $N_r$ species (Gilman et al., 2015; Stockwell et al., 2015; Warneke et al., 2011). A number of studies have sought to summarize both real world and laboratory emissions of $N_r$ compounds (Akagi et al., 2011; Andreae, 2019; Andreae and Merlet, 2001; Coggon et al., 2016; Yokelson et al., 2013b; Yokelson et al., 2009). The known N-compounds range in oxidation state from $NH_3$ to $HNO_3$ and include $N_2$ and $N_2O$. Among the more prominent and important $N_r$ species are: $NO_x$ (NO and $NO_2$) which is a key player in the atmospheric oxidant cycle; $NH_3$ which has a major role in particle formation; HONO which can be an important radical source; HCN and acetonitrile ($CH_3CN$) which are toxic at high concentrations and represent valuable tracers for following fire transport; and isocyanates, HNCO and methyl isocyanate ($CH_3NCO$) which have unique health impacts (Roberts et al., 2011). In addition, nitro ($-NO_2$), or nitrogen heterocyclic compounds may contribute to so-called brown carbon, aerosol organic compounds exhibiting optical absorption in the near-UV or blue wavelength regions. Wildfire N emissions also have very minor contributions from gas phase nitric acid ($HNO_3$). Nitric acid is either not efficiently produced by BB or is readily incorporated into aerosol if it is produced in fresh wildfire plumes, as is clear from the absence of $HNO_3$ enhancements in several studies of BB plumes (Liu et al., 2016; Yokelson et al., 2009)Alvarado et al., 2010), however nitrate ($NO_3^-$) has been shown to contribute to aerosol mass particularly for inefficient combustion (May et al., 2014). Flame chemistry is inefficient in forming $N_2O$, relative to the pathways that form $N_2$ (Andreae, 2019; Andreae and Merlet, 2001; Griffith et al., 1991; Hao et al., 1991). The modeling of the emissions of these N-compounds on a large scale could benefit from a better understanding of the total budget of these species as a function of fuel nitrogen content and the dependence of the individual species on fuel type and combustion conditions.

The construction of $N_r$-budgets in this work is made possible by the inclusion of a total reactive nitrogen measurement (termed $N_r$ herein), a method by which all nitrogen compounds besides $N_2$ and $N_2O$ are converted to NO and detected by NO-$O_3$ chemiluminescence. This technology has been developed by a number of groups, typically using precious metal or NiCr catalysts that have been shown to convert all $N_r$ compounds to NO (and to some extent $NO_2$) at high temperatures (750-825°C) (Hardy and Knarr, 1982; Kashihira et al., 1982; Marx et al., 2012; Roberts et

al., 1988). There are also commercial instruments that incorporate this technology (see for example Thermo Scientific Model 17i). This technique has been applied to gas phase atmospheric measurements, principally to measure $NH_3$ by difference techniques (Saylor et al., 2010; Schwab et al., 2007), and has also been used to observe wildfire plumes that have impacted ambient air measurements (Benedict et al., 2017; Prenni et al., 2014). We have recently developed a platinum/molybdenum oxide $N_r$ catalyst system, and confirmed that it quantitatively converts $N_r$ compounds including all particle-bound nitrogen compounds (Stockwell et al., 2018). To our knowledge this technique has not been applied directly to BB emissions before.

This paper describes the total reactive nitrogen, and individual $N_r$ compound measurements made during the FireLab 2016 experiment, with the intent of providing information that can be used for analysis and modeling of the impact of wildfire emissions on the atmosphere. The total $N_r$ measurements are combined with $CO_2$, CO, and VOC measurements and fuel, residue and ash C and N content to estimate the amount of N lost to $N_2$ and $N_2O$. In addition, systematics of the ratio Nr/Total Carbon are examined for simplifying relationships. Fire-integrated $N_r$ is then compared to fire-integrated measurements of individual compounds to determine the fraction of unaccounted-for $N_r$. The systematic behavior of individual $N_r$ species and their fractional contribution to $N_r$ are examined with respect to fuel type, N content, and combustion processes. A positive matrix factorization (PMF) technique is used to examine commonalities between fires of different fuels under different conditions and compared to the PMF analysis of the VOC emissions published by Sekimoto et al., (2018). The results are used to arrive at suggested guidelines that can be used estimate $N_r$-emissions profiles for fires representative of western North America.

## 2 Methodology

The FireLab 2016 study involved laboratory burns of fuels mostly characteristic of western North American wildfires such as coniferous fuels and chaparral fuels (important in central to southern California and the southwestern U.S.). We also measured some that have global significance such as Indonesian peat and yak dung (important in areas above timberline or where wood is scarce, such as India, Nepal, and Tibet). The procedures and associated details of the study have been described previously by Selimovic et al., (2018) and will be only briefly summarized here. The detailed data on fuel types, amounts and composition can be found in Table S1, and in the Supplemental section of Selimovic, et al., (2018). The laboratory burns involved fuel samples, ranging in mass from 0.26 to 6.02 kg spread out on a fuel bed roughly 1m x1m square. Fires were started without the addition of any contaminants, using an electric igniter (a series of NiCr heating elements that were flash-heated electrically), and typically lasted from approximately 5 to 30 minutes. Seventy-five fires were conducted in the “stack” burn configuration where the smoke was directed up the central stack of the facility where it could be sampled simultaneously by all the instruments that measured gas phase species, and some of the particle phase measurements. The sampling platform was about 15 m above the fire and the sampling took place in well-mixed smoke approximately 5s after emission (Christian et al., 2004). Thirty-one additional fires were conducted as “room” burns on most of the same fuels, when the stack was closed and the room was allowed to fill with smoke, permitting sampling to be done over the course of several hours. The following analyses will focus on the “stack” burns, as those measurements had little or no interferences from surfaces, where “room” burns are known to be compromised by the loss of materials, such as $NH_3$, to the room walls at long sample

times (Stockwell et al., 2014). Ash analyses were performed only on the residues from the room burns and those values will be used for the N and C budget calculations, with the assumption that stack and room burns left similar ash considering the combustion conditions were the same for each type of fire. Table 1 lists the compounds and associated techniques used to measure them during the FireLab 2016 study, and describes the grouping of NVOCs measured by PTR-ToF into common categories, e.g. amines, nitriles, etc. We specifically note that the OP-FTIR is capable of measuring gas phase $HNO_3$ with comparatively good sensitivity (10ppbv detection limit in fires where $N_r$ can be 5 ppmv or more), but $HNO_3$ was not observed above detection limit in any of the fires.

### 2.1 $N_r$ and NO measurements by Chemiluminescence

Total reactive N ($N_r$) was measured by catalytic conversion to NO, followed by $O_3$-chemiluminescence using an instrument described previously (Williams et al., 1998). $N_r$ and NO were sampled from inlets inserted adjacent to the inlet-less open-path Fourier transform infrared spectrometer (OP-FTIR) instrument path during the stack burns (Selimovic et al., 2018), and from a platform approximately 4 m off the floor in the middle of the room during the room burns. The catalyst used for the $N_r$ channel, described in detail by Stockwell et al. (2018), consisted of a 11mm I.D. quartz tube, packed with 36 platinum screens, heated to 750°C. This tube was wrapped with high temperature heating tape and insulated inside a 7cm OD stainless steel tube that was fitted to a bulkhead placed through the wall of the stack. The $N_r$ channel was diluted by a factor of 5:1 (±3%) using a flow of zero air added immediately downstream of the Pt catalyst assembly. NO was sampled through a 6.3mm O.D. stainless steel inlet tube which was placed through the bulkhead directly into the free air stream of the stack and connected to a 50mm Teflon filter holder immediately outside the stack. The transfer lines for the $N_r$ and NO measurements consisted of 6.35mm O.D, 1mm wall thickness PFA tubing of approximately 20 m in length. $N_r$ and NO data were acquired at 1 s frequency, but the flow rate through each inlet was 1 SL $min^{-1}$, resulting in residence time in each inlet of 14 s. This time delay was corrected in the data analysis. Any chemical effects of the inlet on the sampled air stream were negligible since the analytes consisted of only NO and $NO_2$ and those are known to be transmitted by PFA Teflon tubing with essentially no surface effects. However, there were possible effects of the inlets on the temporal features of the measurement through diffusion or turbulent mixing. Those effects were examined through comparison of the temporal variations in the NO signal with the NO measured by the OP-FTIR, and comparison of the $N_r$ signal under smoldering conditions with the $NH_3$ measured by the OP-FTIR. Both of these comparisons showed that the NO and $N_r$ inlets had effective time constants of 4 seconds, somewhat slower than the diffusive relaxation time assuming solely laminar flow. Examples of the estimate of diffusion and dispersion on NO and $N_r$ signals, and the estimate of the effective time constant of these measurements are presented in the Supplemental Information.

The inlet streams were sampled by the NO instrument either directly (NO channel) or after passing through a second catalyst of molybdenum oxide (MoOx) to convert remaining $NO_2$ to NO. The MoOx catalyst consisted of a molybdenum tube at 350°C to which a small flow of $H_2$ (0.8%v/v) was added to control the re-dox state of the surface. Both channels of the instrument were "de-tuned" to keep raw photon count rates below 4 MHz, by turning down the $O_3$ flows and PMT voltages. Calibrations were performed with both a NO standard in $N_2$ (Scott-Marrin) and 10.1 ppmv standard of HCN in nitrogen (Gasco). The Pt catalyst was dismounted from the stack (or room) every few days

and checked for conversion efficiency by the addition of the HCN standard to the inlet. Conversion efficiencies were found to be consistently high (>98%) throughout the entire sampling period (October 5 – November 12, 2016). There were slight background signals (a few tens of ppbv) for both NO and $N_r$ in both the stack and room air prior to and after the burns, and those were subtracted from the fires signals prior to reporting the data. The overall uncertainties in the NO and $N_r$ data were ±10% for each measurement.

**2.2 Other measurements**

Measurements of individual species during the 2016 FireLab study have been presented in several previous publications. The OP-FTIR measurements were discussed by Selimovic et al., 2018, and the PTR-ToF measurements were discussed by Koss et al., (2018). In addition, some of the calibration methods and GC separation and identifications rely on additional analytical work presented by Sekimoto et al., (2017) and Gilman et al., (2015). We measured the mass and elemental content of the initial fuel and the mass of unburned fuel for all the fires, and we measured the mass and the elemental content of the ash during 21 room burns, which covered all the fuel types discussed.

**2.3 PMF Analysis**

Trace gas measurements from multiple instruments involved in the FireLab study were combined and analyzed using positive matrix factorization (PMF). PMF is a numerical method that was used in this case to partition the compounds involved in a time varying mixture of chemicals into a few groups, or "factors", where a compound can appear in more than one factor. A factor represents a consistent profile of compounds that is representative of one of the sources contributing to the total signal. The sum of all the "factors" then ideally describes the total composition of the measurements, which in this case is the emissions of $N_r$ compounds. By its nature, PMF assumes that the total signal is a linear combination of individual sources that have a consistent composition, the relative contribution of which is represented by the amount of each compound or category found in each factor (Paatero and Tapper, 1994; Ulbrich et al., 2009). We hypothesize that species with dominant fractions in the same factor are related to each other via the same formation processes. With knowledge of factor composition and the amount of each factor at any given time the original emissions measurements can be reconstructed and this approach provides an alternate source of profiles for fire emissions. PMF has also been used by a number of groups to explore how much various source profiles contribute to complex ambient measurements (see for example Ulbrich et al., 2009) and was recently used to analyze PTR-ToF-MS measurements from the FireLab (Sekimoto et al., 2018). Here, PMF was accomplished using the PMF Evaluation Tool v. 2.08A (Ulbrich et al., 2009).

The application of PMF to this data set is different than the instances where it is applied to data from a single instrument in which compound abundances are inherently scaled properly and error estimates are well defined and self-consistent. For example, when applied to mass spectral data from a single instrument, errors can be expected to scale as the square root of ion counts based on fundamental counting statistics (Sekimoto et al., 2018). In this work we are including nitrogen measurements from several instruments, thus we chose to use mixing ratios as the unit of comparison. The error estimates required by the PMF analysis were taken from the reported combined uncertainties:

229 the sum of the detection limit plus the estimated random error of the measured value. For example, the uncertainty in
230 a NO mixing ratio of 500ppbv was ±51ppbv. The variables that were used in this PMF analysis and their units and
231 corresponding errors are listed in Table 2. Where compound categories are specified (e.g. nitriles), the values were
232 the sum of the measured compounds in that category as listed in the footnotes to Table 1. The data were further
233 adjusted by subtracting the ambient air background before and after the fires, which was a relatively minor adjustment
234 for most compounds and categories. Any negative numbers that resulted were very small compared to the fire
235 emissions, and were set to zero. In addition to the PMF analysis for the species listed in Table 2, several exploratory
236 runs were tried with $CO_2$, CO added (in units of ppmv) and total $N_r$ (in units of ppbv) added to the list in Table 2. No
237 significant differences were observed in the results for individual $N_r$ compounds and classes, so $CO_2$, CO and Total
238 $N_r$ were not included in this analysis.
239 We applied PMF to single fire data as well as extended time series that included all fires of a particular fuel
240 type, in-line with the approach laid out by Sekimoto et al., 2018. By consolidating fuels from a particular vegetation
241 type, the fire to fire variability largely driven by differences in the fuel (e.g. moisture content, structure, quantity) is
242 constrained and the most representative fire conditions are captured. Two fuel groups were analyzed in this way: the
243 western U.S. coniferous ecosystem fuels which included ponderosa pine, lodgepole pine, Douglas fir, Engelmann
244 spruce, and sub-alpine fir and the Southwestern U.S. chaparral ecosystem which was represented by chamise and
245 manzanita. The consolidated time series for the coniferous ecosystems included realistic mixtures, canopy only, and
246 litter only, while duff and rotten logs were analyzed separately, and not included in the timeseries.
247
248 **3 Results and Discussion**
249 The measurements of total $N_r$ can be combined with N and C measurements of fuel and ash to estimate N
250 lost to $N_2$ and $N_2O$. The total $N_r$ emitted from laboratory fires combined with individual N compound measurements
251 allow us to construct a budget for $N_r$ species that define what the dominant forms of N are and how those emissions
252 depend on other fire parameters, or different temperature combustion processes. The systematics of N emissions found
253 by PMF are compared to other fire indicators and PMF analyses previously conducted on VOCs allow the formulation
254 of simplifying relationships that can be used in atmospheric models of wildfires.
255
256 **3.1 Comparison of $N_r$ and Total Carbon in fire emissions**
257 The total $N_r$ and total carbon emissions were measured for 75 stack fires in order to place the N emissions in
258 the context of total carbon which has be widely estimated for wildfires. Example timeseries of NO, $N_r$, $\Delta CO$, $\Delta CO_2$
259 (CO and $CO_2$ corrected for their backgrounds) are shown in Figure 2, for a fire burning a sample of ponderosa pine
260 realistic mix (Fire 004). In addition to the chemical species, the modified combustion efficiency (MCE) was also
261 plotted. MCE is defined as
262
263 $$MCE = \Delta CO_2/(\Delta CO_2 + \Delta CO) \quad \text{(Eq. 1)}$$
264

where $\Delta CO_2$ and $\Delta CO$ are the $CO_2$ and CO levels above the ambient. MCE has traditionally been used to indicate the relative amount of flaming and smoldering combustion in a fire. The timeseries for Fire 004 (Figure 2) shows a short initial smoldering/distillation phase (MCE 0.7 to 0.8) as heat pyrolyzes the fresh fuel and releases VOCs from existing pools in the fuel followed after ignition by a relatively efficient mix of flaming and smoldering combustion (MCE 0.95 to 0.98) and then finally a subsequent period of essentially pure smoldering (MCE ~0.80). The $N_r$ and NO timelines had many features in common because NO is often the most abundant $N_r$ compound (see below). As a result, it is useful to compare the quantities $N_r$–NO and $(N_r\text{-NO})/N_r$ to the other measures of chemical species or combustion efficiency. As expected, $(N_r\text{-NO})/N_r$, in Figure 2(c) is anti-correlated with MCE since $N_r$ is primarily NO at high MCE. In addition to the anti-correlation, this non-NO fraction, like its approximate carbon analog $CO/CO_2$, has a wider dynamic range than MCE and will often suffer less from background variability than carbon-based indices (Yokelson et al., 2013a).

The concentration profiles of the background-corrected measurements of $N_r$, $CO_2$, CO, and all the carbon-containing species measured by the FTIR (Selimovic et al., 2018) during the stack burns were integrated over the entire time of the burn to obtain total carbon, termed TC here, and total $N_r$. The additional carbon species included methane and a number of other gas phase VOCs as well as organic- and black-carbon aerosol. Altogether these carbon species should account for ≥98% of emitted carbon (McMeeking et al., 2009). Total $N_r$ is plotted in Figure 3, versus TC (Figure 3a) and versus nitrogen burned, which is calculated from the %N in the fuel × the mass of fuel consumed (Figure 3b). The points in Figure 3 are colored by the fuel N/C mole % obtained from the elemental analysis of each fuel. The relationship between $N_r$ and TC in panel 3a clusters around the 0.37% line and those points are from fuels most characteristic of the North American biomes impacted by wildfire. There are clear outliers in the correlation of $N_r$ and TC; for example, yak dung and two samples of duff (Engelmann spruce and subalpine fir) were high due either to the fact that they have high fuel N/C ratios (dung, see Table S1), or they burned with minimal flaming (whole fire MCEs 0.86-0.89, duff and dung), hence experienced less de-nitrification. The fuels that were low in $N_r$/TC in panel 3a, ponderosa pine rotten log, subalpine fir and excelsior, had low fuel N/C, so when plotted versus nitrogen burned in panel 3b, they cluster with the main group of characteristic fuels, i.e. they are no longer 'outliers' in the distribution.

### 3.2 Estimates of denitrification

The removal of N to forms in-active in the troposphere, $N_2$ and $N_2O$, has importance in the biogeochemistry of forest ecosystems and also determines how much N takes part in wildfire plume chemistry. The points in Figure 3a are all lower than the corresponding fuel N/C mole ratio, due to the denitrification chemistry, shown in Figure 1, and verified in lab studies described by Kuhlbusch et al. (1991), and the production of $N_2O$ which is also not measured by the $N_r$ technique. The sum of $N_2$ and $N_2O$ produced in the fires can be estimated from the difference between the fuel N/C and the $N_r$/Total C emitted and the data on C and N content remaining in the ash. The mass balance equations used for these calculations are detailed in the Supplemental Materials.

The distribution of the N lost to $N_2$ and $N_2O$ is shown in Figure 4. Chemical analyses were not done for all fuels during the stack burns, and the analysis above assumes that the ash residues and ash/burned fuel ratios from the stack burns were well represented by those for the same fuels used in the room burns, for which mass yields and

chemical analyses were done. Data are missing for fuels that did not have a corresponding residue analysis. The median fraction of N lost to $N_2$ and $N_2O$ for ash-corrected fires was 0.70, and the mean (±standard deviation) was 0.68 (±0.14). This fuel-based estimate is uncertain by approximately 25% because of the above assumptions concerning the applicability of the residue analyses from the room burns and because fuel moisture corrections were assumed to apply to all of the materials burned, foliage vs. woody biomass (see SI for details). The emission of $N_2O$ relative to $N_2$ is approximately 10% or less for a wide range of fuels (Andreae, 2019). Assuming the N remainder in our work is at least 90% $N_2$ gives values that are somewhat higher than the $N_2$ values reported by Kuhlbusch et al., (1991) where $N_2$ accounted for 36% of fuel N burned in flaming stage fires. A closer inspection of Kuhlbusch et al., (1991) showed a range of $N_2$ yields of 40-54% at highest MCEs of 0.94-0.97. Possible reasons for these differences are that the Kuhlbusch et al., (1991) fires were limited to grasses, hay, and pine needles, and the fires were confined to a closed container and so may not have experienced the convection and turbulence of typical biomass fires. In addition, the fires analyzed in our work were somewhat weighted towards the full canopy and higher temperature burning fuels, since ash analyses were not done for peat, dung and many of the "litter" samples, all of which tend to burn less efficiently. Goode et al., (1999) estimated an $N_2$ emission of 45±5% for MCE values of 0.95 in grass and surface fuels. The range of values determined in our work overlap with these literature values, but are on average higher. It should be noted that such loss of reactive nitrogen can have implications for ecosystem N budgets, as discussed by Kuhlbusch et al., (1991).

### 3.3 The budget of $N_r$ and individual N containing species

The composition of the N that does not get converted to $N_2$ or $N_2O$ is of intense importance in determining atmospheric impacts of fires, since those compounds are involved in oxidation capacity (NOx), radical production (HONO) and particle formation ($NH_3$). Emission factors for all the individual $N_r$ compounds identified in our work have been compiled and reported in previous publications (Koss et al., 2018; Selimovic et al., 2018), so this paper will focus on the $N_r$ budget. The balance of $N_r$ budget for Fire 047, sub-alpine fir realistic mix, is shown in Figure 5, in which the timelines of $N_r$, NO, $N_r$-NO, sumN, and NVOC are plotted along with MCE and $(N_r\text{-NO})/N_r$. The quantity sumN is the sum of all other non-NO compounds, and NVOC is the subset of sumN that are organic nitrogen compounds measured by the PTR-ToF, as listed in Table 1. This fire had a mixture of flaming and smoldering combustion throughout the fire as indicated by MCE and nitrogen profiles (panel (d)). The comparison of $N_r$-NO with the sumN in panel (b) shows that much of the N is accounted for. The major contributors to sumN for this fire were HNCO, HCN, HONO, $NO_2$, and $NH_3$, while NVOC was a very small contributor to sumN (panel (b)). Note that while $HNO_3$ is measurable by FTIR with good sensitivity, no $HNO_3$ signals were observed above detection limit, which was 10 ppbv. Panel (c) shows the residual left after NO and sumN are subtracted from $N_r$, corresponding to an integrated amount of 15.6 ±8% of $N_r$. This residual is reasonable considering typical published particle $N_r$ measurements (Akagi et al., 2012; Akagi et al., 2011; Liu et al., 2017; May et al., 2014), and consistent with there being some particle $N_r$ from flaming, which are most likely organic nitrates or nitro-organics, and particle ammonium from smoldering with potassium or ammonium nitrate potentially accounting for substantial $N_r$.

Several fuels had much lower NO emissions and higher unaccounted for $N_r$. Yak dung was one such fuel the emissions of which stand in contrast to the fire shown above. The nitrogen emissions from Fire 050, yak dung, are

shown in Figure S2. This fuel produced mostly smoldering emissions as exemplified by the low NO levels relative to $N_r$ (panel a), and the low MCEs observed (panel d). The sum of $N_r$ species was somewhat correlated with the quantity $N_r$-NO, but was substantially lower, and the residual $N_r$ unaccounted for by the gas-phase measurements was 33.9 ±16% of $N_r$ (panel c). The majority of sumN was represented by HCN and $NH_3$, with acetonitrile ($CH_3CN$) higher than any of the other inorganics, HNCO, $NO_2$ or HONO. The NVOCs were also a larger fraction of $N_r$-NO than in the case of Fire 047 shown above, a feature that implies that more semi-volatile organic compounds, SVOC, survive these types of fires and could make a proportionally higher contribution to the $N_r$ budget in this fire relative to Fire 047. FireLab results of particle organic carbon measurements (Jen et al., 2019) and field measurements in environments with a lot of dung burning (Jayarathne et al., 2018; Stockwell et al., 2016a) are consistent with a higher EF for particle organic carbon and by extension particle NVOC compounds. The quantity ($N_r$-NO)/$N_r$ was relatively high and had less dynamic range than for fires with more flaming combustion like Fire 047.

An overall budget of $N_r$ can be constructed for all of the stack fires through integrating the time profile of all the compounds and compound classes. The fire-integrated measurements of inorganic and NVOC species are listed in the Supplemental section as ratios to $N_r$ for each stack fire (Table S1). The summary of all the fire integrated $X_i/N_r$ fractions (where $X_i$ is the $N_r$ species or quantity) is given in Table 3 for all the fires for which we have a complete set of measurements (43 fires). In general, NO was the major species followed by $NH_3$, and the other inorganic $N_r$ species, $NO_2$, HNCO, HONO, and HCN had individual contributions of 4.3 to 9.4 %. NVOC species were less than 5% of $N_r$ on average. The unaccounted-for $N_r$, defined as ($N_r$-NO-sumN)/$N_r$ had a median value of 14.3% and a mean (±std. dev.) of 15 (±10)%. Overall, 85% of $N_r$ was accounted for by the gas phase measurements. The distribution of whole fire $N_r$ residuals is plotted as a histogram in Figure 6. We expect the residual $N_r$ was composed of either semi- or low-volatility compounds, or particle-bound $N_r$ compounds, which we know are converted efficiently by the $N_r$ catalyst (Stockwell et al., 2018) but not detected by the instruments included in this analysis. Along these lines, there is some indication that the residual has a systematic variation with whole fire MCE, with higher residuals (up to 30%) observed at lower MCEs and higher ($N_r$ – NO)/$N_r$ (see Figure S1 a&b), which would be consistent with higher EF for SVOC at low MCE (Jen et al., 2019) and particle $N_r$ having a higher contribution from $NO_3^-$ (May et al., 2014), and perhaps particle ammonium or reduced-$N_r$ compounds. In general, there is more particulate organic material emitted from fires at low MCE (Jen et al., 2019), so we would expect more particle N at low MCE to go along with that.

### 3.4 Systematic dependences of $N_r$ composition on combustion processes.

The features noted in fires shown above, as well as the anti-correlation of MCE and ($N_r$-NO)/$N_r$ lead to the question of whether there are systematic dependences in $N_r$-compound composition on fire stage that can be used to formally classify and/or potentially predict the relative emissions of $N_r$ compounds. MCE has been used as a rough indicator of the relative amounts of flaming and smoldering combustion in a fire, with high MCE (~99%) being "pure" flaming, low MCE (~80%) being "pure smoldering," and an MCE of ~0.9 being roughly equal amounts of both (Sect. 2.1.1 in Akagi et al., 2011). It should be understood that "smoldering" in this framework is a lumped term that includes all non-flame processes such as pyrolysis, glowing, and distillation, which are the processes that produce gaseous fuel to support flaming (Yokelson et al., 1996). In addition, "pure flaming" is essentially the efficient oxidation of

smoldering products before they enter the atmosphere. However, for MCE to predict flaming and smoldering $N_r$ species well, the variable fuel N must be considered. For instance, $NO_x$ is clearly produced by flaming based on its temporal profile, but fire-integrated $EF_{NOx}$ may not correlate with MCE due to variable fuel N. In these cases, $EF_{NOx}$/fuel N or $\Delta NH_3/\Delta NOx$ may still correlate (or anti-correlate) well with MCE (e.g. Fig. 4 in Burling et al., 2010 or Yokelson et al., 1996). Finally, the flame chemistry involving $NH_3$, HNCO, and HCN both produces and destroys NO in a fashion that does not conserve $N_r$. This chemistry is explored in Figure 7 in which NOx, $NH_3$, HNCO, HCN, HONO, and $CH_3CN$ ratios to $N_r$ are plotted vs real-time MCE for Fire 047 as a typical example for fires that have a substantial range of MCEs (e.g. from 0.8 to above 0.98). The relationship between $NH_3/N_r$ and MCE confirms that $NH_3$ is primarily a smoldering emission and $NO_x/N_r$ increases with increasing MCE in a non-linear fashion that confirms it is primarily a flaming compound. Such a non-linear dependence has also been seen for other flaming-related quantities such as Elemental Carbon/TC or $EF_{HCl}$ (Christian et al 2003; Stockwell et al., 2014). Most importantly, the variations of $HNCO/N_r$, $HCN/N_r$, $HONO/N_r$, and $CH_3CN/N_r$ versus MCE do not arise dominantly from either regime as these are species that are likely produced by multiple pathways (e.g. "incomplete flaming", pyrolysis, possibly glowing). By "incomplete" flame chemistry we mean the production of incompletely oxidized products in flames such as the complex system of reactions shown in Fig. 1. These reactions involving HNCO, HCN and $NH_3$ both produce and destroy NO, while HONO is produced from reactions of NO and $NO_2$ that are faster at slightly lower temperatures, for example the three-body association reaction of NO with OH radical (Manion et al., 2015). Variable turbulence in the turbulent diffusion flames that are characteristic of open BB likely contributes to varying temperatures, and therefore, varying amounts of incomplete oxidation of the fuel N (Shaddix et al., 1994).

### 3.5 The PMF analysis of coniferous fuels

The complexity of the dependence of $N_r$ speciation on combustion chemistry suggests that MCE is an insufficient model to use for applying lab results to real-world fire emissions (Stockwell et al., 2016a; Yokelson et al., 2013b). Accordingly, we employed the positive matrix factorization (PMF) method (see Methodology section) that has been used by a number of groups to probe the sources contributing to complex mixtures (see for example Ulbrich et al., 2009 Sekimoto et al., 2018). Our PMF results showed several general features, irrespective of the inclusion or exclusion of $CO_2$, CO and $N_r$. The emissions were best fit by three factors (with approximate descriptive names justified below and prime species): (1) a combustion (flaming) factor (abbreviated Comb-N), (2) a high temperature pyrolysis factor (HT-N), and (3) a low temperature pyrolysis factor, (LT-N). We use these terms in part to harmonize our discussion with the VOC results discussed by Sekimoto 2018. An example timeseries for the PMF analysis of a coniferous fuel with just the $N_r$ species included is shown in Figure 8 for a realistic mix of lodgepole pine (Fire 063). In this case, several different Fpeak values were tried (-1, 0, +1) and runs with 100 different seeds (initial factor profiles) were performed. The results of those analyses (Figure S4) show that a 3-factor PMF result is robust. A PMF analysis was performed on the consolidated time series of all coniferous fuels fit using just the $N_r$ species, as shown in Figure S5. In this case Fpeak=0 was used and the Q/Qexpected showed an inflection for the 3-factor solution at a value of 5.3 The three factors successfully describe the majority of the $N_r$-emissions where the difference between the

412 measured and calculated mass is on average 5.1% for coniferous fuels and 4.6% for chaparrals as indicated in Table
413 4.

414 Several metrics of the PMF analysis quantify how the compounds or compound classes contribute to each
415 factor. The 'loadings' of the three different factors, i.e. the contribution of compounds to each factor, for coniferous
416 fuels are shown in Figure 9(a), and the distribution of a given compound or compound class amongst the three factors
417 is shown in Figure 9(b) as normalized fraction. Normalized fraction is equal to the PMF-determined contribution of a
418 compound to a factor, divided by the sum of the contribution of the compound to all three factors. The Comb-N factor
419 contained NO, $NO_2$, and HONO, the HT-N factor had mostly HCN, HNCO, nitriles, with contributions from $NO_2$ and
420 nitro compounds, and the LT-N factor contained $NH_3$, amines, amides and heterocyclics. Within the Comb-N factor
421 there is some evidence that the relative amounts of HONO and NOx depend on fuel moisture. For example, the ratio
422 HONO/NOx for whole fires shows some correlation with needle moisture in coniferous fires that were canopy fuels
423 (Foliage and small woody biomass), as shown in Figure S6. This may be due to flame processes that interconvert NOx
424 and HONO in the presence of water vapor of OH (see Figure 1).

425 Literature values from studies where flame temperature was measured are typically in the range of 1100 –
426 1200 °C (Taylor et al., 2004; Wotton et al., 2012), so we would assume that would constitute the upper range of our
427 Comb-N factor. The radical chemistry involving HCN, HNCO and $NH_3$ starts to shut down below about 800-900°,
428 according to the modeling of Glarborg et al., (2018), so we set 800°C as a lower limit for the Comb-N factor. The HT-
429 N factor species are known to be produced by the intense pyrolysis of fuel $N_r$ compounds (Hansson et al., 2004; Liu
430 et al., 2018; Ren et al., 2010), which for these compounds becomes important at temperatures around 500-600°C.
431 Accordingly, we estimate the temperature range for the HT-N factor at 500 – 800°C. The remaining LT-N factor
432 results from mild pyrolysis and pertains to fire conditions of roughly 500°C and below, and was dominated by $NH_3$,
433 amines, amides and some of the more complex organics (Koss et al., 2018). The names and temperature ranges are
434 approximate and likely include processes that occur inside flames as part of the flame proper, as turbulent diffusive
435 flames are highly variable in space and time.
436

437 **3.6 The comparison of N-PMF factors to other fire parameters and VOC emission factors.**

438 It is useful to explore the correlation of N-PMF factors with other fire indicators to determine relationships
439 for parameterizing $N_r$ emissions together with carbon and VOC emissions, in order to simplify how emissions might
440 be parameterized in models. The Comb-N factor for coniferous fuels, which consisted of $NO_x$ and HONO, would be
441 expected to correlate with $CO_2$ but not as well with MCE since the latter includes an indicator of incomplete
442 combustion. The timeseries of Comb-N along with $CO_2$ and with MCE for Fire 037 (ponderosa pine), are plotted in
443 Figure 10. As expected they show an excellent correlation of Comb-N with $CO_2$ ($R^2$=0.942) since all the species are
444 flaming compounds, but non-linear correlation of Comb-N with MCE ($R^2$=0.363) since the latter factors in a
445 smoldering compound (CO), similar to the $NOx/N_r$ vs. MCE plot for Fire 047 in Figure 7. The excellent correlation
446 of Comb-N with $CO_2$ is a broadly applicable result, the $R^2$ parameters for all the fires shown in Figure S5 had an
447 average of 0.898, and ranged from 0.806 to 0.966. As a consequence, we can conclude that $CO_2$ would be the best

tracer for Comb-N in many western U.S. ecosystems where conifers predominate, provided ambient $CO_2$ backgrounds can be properly accounted for as described by Yokelson et al., (2013a).

Our Comb-N factor did not correspond to the high temperature VOC factor (HT-VOC) found by Sekimoto et al., (2018) in their pyrolysis study because our broader study includes flaming combustion, which produces NOx, and HONO, and almost none of the compounds classified as VOCs survive flaming conditions. However, the HT-N and HT-VOC factors are both linked to pyrolysis and were well correlated for many fires. An example of this is shown in Figure 11 for Fire 037, a sample that was broadly representative of ponderosa pine (i.e. canopy and litter). This result can be rationalized by the fact that while HT-VOC factors have large contributions from many more compounds that the N compounds measured here, they also have large contributions (>85%) from HCN, HNCO, and HONO, (in other words >85% of HCN, HNCO and HONO are found in the HT-VOC factor). Since the HT-N factors are also heavily weighted by HCN and HNCO, it is reassuring that both of these PMF analyses have independently identified these species as important contributors to the HT fire regime. The $R^2$ correlation coefficients between the HT-N and HT-VOC factors for the coniferous fires shown in Figure S5 averaged 0.866 and ranged from 0.419 to 0.959. As a consequence of this correlation, we can conclude that HCN is the best marker for the HT-N and HT-VOC factors in most western U.S. wildfires, since HCN is essentially inert on the timescales of fire plumes (Li et al., 2000). It should be noted that other nitriles, particularly acetonitrile, also show up in the HT-N factor, and acetonitrile has also been used as a tracer of biomass combustion. However, it has been shown that this acetonitrile signal can be obscured in urban or industrial areas by solvent usage, or can be quite small in woodstove emissions due to low N in the fuel (Coggon et al., 2016).

The correlations of LT-N and LT-VOC factors were not particularly high for most of the coniferous fires shown in Figure S5. The average $R^2$ was 0.427 with a range of between 0.072 and 0.827. The reasons for this lack of correlation are not clear, as $NH_3$, amines and amides appear predominantly in both LT factors, and the absolute concentrations of $NH_3$ are usually quite high in these fires relative to VOCs (Sekimoto et al., 2018). However, the LT-VOC factor includes many more compounds with a variety of functional groups not found in the LT-N factor, so it appears that the VOC and N compounds have sufficiently different pyrolysis chemistry that the LT factors do not show much correlation. We conclude that $NH_3$ (and particle $NH_4^+$) will be the best marker for the LT-N factor in western U.S. coniferous wildfires, but the LT-VOC chemistry might not be captured reliably by this marker.

**3.7 PMF analysis of chaparral fuels.**

Chaparral is an important ecosystem of concern in wildfires that occur in central and southern California, and other areas of the southwestern U.S. The emissions from burning chaparral fuels (manzanita and chamise) collected at two sites in California were also analyzed as a group and yielded three separate factors in a fashion similar to the coniferous fuels (see Figure S7 for the PMF timeline). As with the coniferous fuels, there was essentially no change in the 3-factor solution with Fpeak, so Fpeak 0 was used, and the Q/Qexp was 3.8. The chaparral factors had slightly different composition (Figure S8), the combustion factor was mostly NO, with small amounts of HNCO, HONO and $NH_3$, the high temperature factor was dominated by $NO_2$ and included HONO, HCN, and HNCO, and the

low temperature factor was mostly $NH_3$ with a slight amount of NO contributing. The NVOC species were found in both the medium and low temperature factors.

There was less similarity between the Comb-N factor and $CO_2$ emissions for chaparral fuels compared to those found for coniferous fuels, with an average correlation coefficient ($R^2$) of 0.689, with a range from 0.244 and 0.950. As a result, there may not be a simple conserved tracer for the combustion factor of these fuel types, however total odd nitrogen (NOy) which is NOx and all the compounds that are produced from NOx in the troposphere, may be useful as it is a reasonably conserved tracer in the absence of wet or dry deposition of particles. Correlation coefficients between the HT-N and HT-VOC factors were on average $R^2 = 0.551$, with a range 0.047-0.911. The correlations between LT-N and LT-VOC factors were in the same range for chaparral fuels as for coniferous, average $R^2 = 0.447$, range 0.028-0.827.

There were some fuels that do not sustain flaming combustion well, specifically duff, Yak dung and Indonesian peat. These fires exhibited little or no NO emission commensurate with minimal flaming combustion. Instead the emissions were mostly the pyrolysis products $NH_3$, (0.22 – 0.53 $N_r$ fraction), and HCN (up to 0.32 $N_r$ fraction for peat). It was also apparent that these fires also had unaccounted for $N_r$, close to, or just over 0.30 (Table S1). The distribution of $N_r$ compounds in the one peat fire that we measured (Fire 055) is in line with those reported for fires measured in situ which showed relatively high EFs for HCN and $NH_3$ (Stockwell et al., 2016b; Stockwell et al., 2015).

### 3.8 Application to real-world fires.

The application of our $N_r$ emissions results to real-world fires will depend somewhat on the nature of the information available on a particular fire, or fire complex. As a good starting point, or in the absence of detailed N and C analyses of fuels, a $N_r$/C ratio of 0.37% appears to capture most of the fires studied in this work. The $N_r$ could be apportioned according to the results summarized in Table 3. Adjustments to those fractions can be made either by scaling slightly by average MCE, with the knowledge that intermediate species (HT-N pyrolysis species) such as HCN and HNCO do not scale in the simple manner that $NH_3$ and $NO_x$ do. If measurements of marker compounds are available then $CO_2$, HCN, and the sum $NH_3 + NH_4^+$ can be used for the combustion, high-temperature pyrolysis, and low-temperature pyrolysis factors respectively.

## 4 Conclusions

Seventy-five stack fire experiments were conducted during the FIREX FireLab experiments in Fall, 2016. A range of fuels characteristic of the western U.S. was burned under conditions and in mixtures meant to represent authentic wildfire conditions, as closely as is possible in the laboratory. Total reactive nitrogen ($N_r$ = all N-containing compounds except $N_2$ and $N_2O$) was measured along with a suite of N-containing compounds in order to obtain a budget for $N_r$-emissions and to examine relationships between fuels, combustion conditions, and emissions chemistry.

Natural convection wildfires do not burn hot enough to produce $NO_x$ from $N_2$ and $O_2$, so all $N_r$ emissions come from the fuel N. Almost all of the fires representative of North American ecosystems had emissions that clustered around a $N_r$/C ratio of 0.37%, which can serve as a starting point for scaling emissions from these ecosystems. Comparing total $N_r$ and total carbon emissions with the N/C ratios of both the original fuel and remaining ash allowed

us to estimate that an average of 68% (±14%) of the fuel nitrogen ends up as $N_2$ and $N_2O$. This loss of nitrogen can be used to estimate how much fuel nitrogen ends up as $N_r$. Of the remaining N emitted as $N_r$, approximately 85% (±10%) was accounted for by individually measured gas-phase species, while the rest was most likely particle-bound $NH_4^+$ and $NO_3^-$, with a smaller contribution from low-volatility species or other species such as cyanogen (Lobert and Warnatz, 1993), that were not quantified by the instruments for individual measurements we used in this study. The speciation and modeling of Nr we present promotes accurate modeling of fire plume chemistry since the photochemistry of many fire plumes is NOx-limited, and $NH_3$ is an important contributor to particle chemistry.

The individual $N_r$ species composition normalized to Total $N_r$, to account for fuel N variability, correlated monotonically with flaming versus vs. smoldering combustion as indicated by modified combustion efficiency (MCE) for some species (e.g. $NH_3$, $NO_x$). Other species, such as HCN and HNCO, peaked at intermediate MCE values. Positive matrix factorization (PMF) showed that all the measured $N_r$ emissions from the main two categories of fuels, conifers and chaparral, grouped into three mixtures (factors), roughly attributed to temperature: combustion (NOx, HONO), high temperature (HNCO, HCN, nitriles), and low temperature ($NH_3$, amines, amides). Chemical kinetic and pyrolysis considerations set the temperature ranges for these regimes at approximately 800-1200°C, 500-800°C and <500°C respectively.

This paper connects mechanistic aspects of N combustion chemistry to the budget of $N_r$ emissions from biomass burning. The emission composition measurements detailed here give useful information concerning what the initial conditions will be in actual fire plumes. These results suggest that for coniferous fuels characteristic of the western U.S. $CO_2$ is the best marker for flaming combustion, HCN is the best marker for high temperature pyrolysis processes, and $NH_3/NH_4^+$ is the best marker for low temperature pyrolysis processes. The HT-N and HT-VOC pyrolysis factors showed high degree of correlation especially for coniferous fuels, which can simplify how these different classes of emissions can be estimated. Results from less comprehensive field experiments can be combined with this emissions information to improve the representation of $N_r$-chemistry in the modeling frameworks needed to predict fire plume chemistry and impacts.

**Data availability**

The FIREX Firelab 2016 data are available at: https://esrl.noaa.gov/csd/groups/csd7/measurements/2016firex/FireLab/DataDownload/. The descriptions of the measurements can be found here: https://esrl.noaa.gov/csd/groups/csd7/measurements/2016firex/FireLab/dataidtable.html. The complete ash analyses are available on request.

**Author Contributions**

JMR, RY, CW and JdG designed the research. The measurements were conducted by JMR, CS, CW, RJY, JdG, YL, VS, ARK, KS, MMC, BY, KJZ, SSB, CS, and SHD. All authors contributed to the discussion and interpretation of the results and writing the paper.

**Competing interests**

Joost de Gouw worked as a consultant for Aerodyne Research during part of the preparation phase of this paper.

## Disclaimer

Any mention of brand names or manufacturers is for information purposes only and does not constitute an endorsement.

## Acknowledgements

A. Koss acknowledges funding from the NSF Graduate Fellowship Program. K. Sekimoto acknowledges funding from the Postdoctoral Fellowships for Research Abroad from Japan Society for the Promotion of Science (JSPS) and a Grant-in-Aid for Young Scientists (B) (15K16117) from the Ministry of Education, Culture, Sports, Science and Technology of Japan. R. Yokelson and V. Selimovic were supported by NOAA-CPO grant NA16OAR4310100. J. de Gouw was supported by the NSF AGS grant 1748266 under a subcontract to the University of Montana during the analysis phase of this work. We thank the USFS Missoula Fire Sciences Laboratory for their help in conducting these experiments, especially Shawn Urbanski and Thomas Dzomba. This work was also supported by NOAA's Climate Research and Health of the Atmosphere Initiatives.

## References

Abatzoglou, J. T. and Williams, A. P.: Impact of anthropogenic climate change on wildfire across western US forests, Proc. Natl. Acad. Sci., 113, 11770-11775, 2016.

Akagi, S. K., Craven, J. S., Taylor, J. W., McMeeking, G. R., Yokelson, R. J., Burling, I. R., Urbanski, S. P., Wold, C. E., Seinfeld, J. H., Coe, H., Alvarado, M. J., and Weise, D. R.: Evolution of trace gases and particles emitted by a chaparral fire in California, Atmos. Chem. Phys., 12, 1397-1421, 2012.

Akagi, S. K., Yokelson, R. J., Wiedinmyer, C., Alvarado, M. J., Reid, J. S., Karl, T., Crounse, J. D., and Wennberg, P. O.: Emission factors for open and domestic biomass burning for use in atmospheric models, Atmos. Chem. Phys., 11, 4039-4072, 2011.

Alvarado, M. J., Logan, J. A., Mao, J., Apel, E., Riemer, D., Blake, D., Cohen, R. C., K.-E., M., Perring, A. E., Browne, E. C., Wooldridge, P. J., Diskin, G. S., Sachse, G. W., Fuelberg, H., Sessions, W. R., Harrington, D. L., Huey, L. G., Liao, J., Case-Hanks, A., Jimenez, J. L., Cubison, M. J., Vay, S. A., Weinheimer, A. J., Knapp, D. J., Montzka, D. D., Flocke, F. M., Pollack, I. B., Wennberg, P. O., Kurten, A., Crounse, J. D., St. Clair, J. M., Wisthaler, A., Mikoviny, T., Yantosca, R. M., Carouge, C. C., and Le Sager, P.: Nitrogen oxides and PAN in plumes from boreal fires during ARCTAS-B and their impact on ozone: an integrated analysis of aircraft and satellite observations, Atmos. Chem. Phys., 10, 9739-9760., 2010.

Andreae, M. O.: Emission of trace gases and aerosols from biomass burning – an updated assessment, Atmos. Chem. Phys., 19, 8523-8546, 2019.

Andreae, M. O. and Merlet, P.: Emission of trace gases and aerosols from biomass burning, Global Biogeochem. Cycles, 15, 955-966, 2001.

Benedict, K. B., Prenni, A. J., Carrico, C. M., Sullivan, A. P., Schichtel, B. A., and Collett Jr., J. L.: Enhanced concentrations of reactive nitrogen species in wildfire smoke, Atmos Environ., 148, 8-15, 2017.

Burling, I. R., Yokelson, R. J., Griffith, D. W. T., Johnson, T. J., Veres, P., Roberts, J. M., Warneke, C., Urbanski, S. P., Reardon, J., Weise, D. R., Hao, W. M., and de Gouw, J.: Laboratory measurements of trace gas emissions from biomass burning of fuel types from the southeastern and southwestern United States, Atmos. Chem. Phys., 10, 11115-11130, 2010.

Christian, T. J., Kleiss, B., Yokelson, R. J., Holzinger, R., Crutzen, P. J., Hao, W. M., Shirai, T., and Blake, D. R.: Comprehensive laboratory measurements of biomass-burning emissions: 2, First intercomparison of open path FTIR, PTR-MS, GC-MS/FID/ECD, J. Geophys. Res., 109, D02311, 2004.

Coggon, M., Veres, P. R., Yuan, B., Koss, A. R., Warneke, C., Gilman, J. B., Lerner, B., Peischl, J., Aikin, K., Stockwell, C. E., Hatch, L. E., Ryerson, T. B., Roberts, J. M., Yokelson, R. J., and de Gouw, J.: Emissions of nitrogen-containing organic compounds from the burning of herbaceous and arboraceous biomass: fuel composition dependence and the variability of commonly used nitrile tracers, Geophys. Res. Lett., 43, 9903-9912, 2016.

Crutzen, P. J. and Andreae, M. O.: Biomass burning in the tropics: Impact on atmospheric chemistry and biogeochemical cycles, Science, 250, 1669-1678, 1990.

Gilman, J. B., Lerner, B. M., Kuster, W. C., Goldan, P. D., Warneke, C., Veres, P. R., Roberts, J. M., deGouw, J. A., Burling, I. R., and Yokelson, R. J.: Biomass burning emissions and potential air quality impacts of volatile organic compounds and other trace gases from temperate fuels common to the United States, Atmos. Chem. Phys., 15, 13915-13938, 2015.

Glarborg, P., Miller, J. A., Ruscic, B., and Klippenstein, S. J.: Modeling nitrogen chemistry in combustion, Prog. Energy Comb. Sci., 67, 31-68, 2018.

Griffith, D. W. T., Mankin, W. G., Coffey, M. T., Ward, R. E., and Riebau, A.: FTIR remote sensing of biomass burning emissions of $CO_2$, CO, $CH_4$, $CH_2O$, NO, $NO_2$, $NH_3$, and $N_2O$. In: Global Biomass Burning: Atmospheric, Climatic, and Biospheric Implications, Levine, J. S. (Ed.), The MIT Press, Cambridge, MA, 1991.

Hansson, K.-M., Samuelsson, J., Tullin, C., and Amand, L.-E.: Formation of HNCO, HCN, and $NH_3$ from the pyrolysis of bark and nitrogen-containing model compounds, Combust. Flame, 137, 265-277, 2004.

Hao, W. M., Scharffe, D. H., Lobert, J. M., and Crutzen, P. J.: Emissions of $N_2O$ from the burning of biomass in an experimental system, Geophys. Res. Lett., 18, 999-1002, 1991.

Hardy, J. E. and Knarr, J. J.: Technique for measuring the total concentration of gaseous fixed nirogen species, J. Air Pollut. Contr. Assoc., 32, 376-379, 1982.

Jayarathne, T., Stockwell, C. E., Bhave, P. V., Praveen, P. S., Rathnayake, C. M., Islam, M. R., Panday, A. K., Adhikari, S., Maharjan, R., Goetz, J. D., DeCarlo, P. F., Saikawa, E., Yokelson, R. J., and Stone, E. A.: Nepal Ambient Monitoring and Source Testing Experiment (NAMaSTE): emissions of particulate matter from wood- and dung-fueled cooking fires, garbage and crop residue burning, brick kilns, and other sources, Atmos. Chem. Phys., doi: 10.5194/acp-18-2259-2018, 2018. 2259-2286, 2018.

Jen, C. N., Hatch, L. E., Selimovic, V., Yokelson, R. J., Weber, R., Fernandez, A. E., Kreisberg, N. M., Barsanti, K. C., and Goldstein, A. H.: Speciated and total emission factors of particulate organics from burning western US wildland fuels and their dependence on combustion efficiency, Atmos. Chem. Phys., 19, 1013-1026, 2019.

Kashihira, N., Makino, K., Kirita, K., and Watanabe, Y.: Chemiluminescent nitrogen detector-gas chromatotography and its application to measurement of atmospheric ammonia and amines, J. Chromatogr., 239, 617-624, 1982.

Koss, A. R., K., S., Gilman, J. B., Selimovic, V., Coggon, M. M., Zarzana, K. J., Yuan, B., Lerner, B. M., Brown, S. S., Jimenez, J. L., J., K., Roberts, J. M., Warneke, C., Yokelson, R. J., and de Gouw, J.: Non-methane organic gas emissions from biomass burning: identification, quantification, and emission factors from PTR-ToF during the FIREX 2016 laboratory experiment, Atmos. Chem. Phys., 18, 3299-3319, 2018.

Kuhlbusch, T. A., Lobert, J. M., Crutzen, P. J., and Warneck, P.: Molecular nitrogen emissions from denitrifcation during biomass burning, Nature, 351, 135-137, 1991.

Lee, B. H., Lopez-Hilfiker, F. D., Mohr, C., Kurten, T., Worsnop, D. R., and Thornton, J. A.: An Iodide-Adduct High-Resolution Time-of-Flight Chemical-Ionization Mass Spectrometer: Application to Atmospheric Inorganic and Organic Compounds,, Environ. Sci. Technol., 48, 6309-6317., 2014.

Lee, D. C., Quigley, T. M., Norman, S., Christie, W., Fox, J., Rogers, K., and Hutchins, M.: National Cohesive Wildland Fire Management Strategy, U.S. Department of the Interior, Washington, D.C., 2014.

Lerner, B. M., Gilman, J. B., Aikin, K. C., Atlas, E. L., Goldan, P. D., Graus, M., Hendershot, R., Isaacman-VanWertz, G. A., Koss, A. R., Kuster, W. C., Lueb, R. A., McLaughlin, R. J., Peischl, J., Sueper, D. T., Ryerson, T. B., Tokarek, T. W., Warneke, C., Yuan, B., and deGouw, J. A.: An improved, automated whole air sampler and gas chromatography mass spectrometry analysis system for volatile organic compounds in the atmosphere, Atmos. Meas. Tech., 10, 291-313, 2017.

Liu, X., Huey, L. G., Yokelson, R. J., Selimovic, V., I.J., S., Muller, M., Jimenez, J. L., Campuzano-Jost, P., Beyersdorf, A. J., Blake, D. R., Butterfield, Z., Choi, Y., Crounse, J. D., Day, D. A., Diskin, G. S., Dubey, M. K., Fortner, E., Hanisco, T. F., Hu, W., King, L. E., L., K., Meinardi, S., Mikoviny, T., Onasch, T. B., Palm, B. B., Peischl, J., Pollack, I. B., Ryerson, T. B., Sachse, G. W., Sedlacek, A. J., Shilling, J. E., Springston, S. R., St. Clair, J. M., Tanner, D. J., Teng, A. P., Wennberg, P. O., Wisthaler, A., and Wolfe, G. M.: Airborne measurements of western U.S. wildfire emissions: Comparison with presscribed burning and air quality implications, J. Geophys. Res., 122, 6108-6129, 2017.

Liu, X., Luo, Z., Yu, C., Jin, B., and Tu, H.: Release mechanism of fuel-N into $NO_x$ and $N_2O$ precursors during pyrolysis of rice straw, Energies, 11, 520, 2018.

Liu, X., Zhang, Y., Huey, L. G., Yokelson, R. J., Wang, Y., Jimenez, J. L., Campuzano-Jost, P., Beyersdorf, A. J., Blake, D. R., Choi, Y., St. Clair, J. M., Crounse, J. D., Day, D. A., Diskin, G. S., Fried, A., Hall, S. R., Hanisco, T. F., King, L. E., Meinardi, S., Mikoviny, T., Palm, B. B., J., P., A.E., P., Pollack, I. B., Ryerson, T. B., Sachse, G. W., Schwarz, J. P., Simpson, I. J., Tanner, D. J., Thornhill, K. L., Ullman, K., Weber, R. J., Wennberg, P. O., Wisthaler, A., Wolfe, G. M., and Ziemba, L. D.: Agricultural fires in the southeastern U.S. during SEAC$^4$RS: Emissions of trace gases and particles and evolution of ozone, reactive nitrogen, and organic aerosol, J. Geophys. Res., 121, 7383-7414, 2016.

Lobert, J. M., Scharffe, D. H., Hao, W.-M., Kuhlbusch, T. A., Seuwen, R., Warneck, P., and Crutzen, P. J.: Experimental evaluation of biomass burning emissions: Nitrogen and carbon containing compounds. In: Global Biomass Burning: Atmospheric, Climatic, and Biospheric Implications, Levine, J. S. (Ed.), The MIT Press, Cambridge, MA, 1991.

Lobert, J. M., Scharffe, D. H., Hao, W. M., and Crutzen, P. J.: Importance of biomass burning in the atmospheric budgets of nitrogen-containing gases, Nature, 346, 552-554, 1990.

Lobert, J. M. and Warnatz, J.: Emissions from the combustion process in vegetation. In: Fire in the Environment: The Ecological, Atmospheric and Climatic Importance of Vegetation Fires, Crutzen, P. J. and Goldhammer, J. G. (Eds.), John Wiley and Sons, New York, N.Y., 1993.

Li, Q., Jacob, D. J., Bey, I., Yantosca, R. M., Zhao, Y., Kondo, Y., and Notholt, J.: Atmospheric hydrogen cyanide (HCN): Biomass burning sources, ocean sink?, Geophys. Res. Lett., 27, 357-360, 2000.

Lucassen, A., Zhang, K., Warkentin, J., Mashammer, K., Glarborg, P., Marshall, P., and Kohse-Hoinghaus, K.: Fuel-nitrogen conversion in the combustion of small amines using dimethylamine and ethylamine as biomass-related model fuels, Combust. Flame, 159, 2254-2279, 2012.

Manfred, K. M., Washenfelder, R. A., Wagner, N. L., Adler, G., Erdesz, F., Womack, C. C., Lamb, K. D., Schwarz, J. P., Franchin, A., Selimovic, V., Yokelson, R. J., and Murphy, D. M.: Investigating biomass burning aerosol morphology using a laser imaging nephelometer, Atmos. Chem. Phys., 18, 1879-1894, 2018.

Manion, J. A., Huie, R. E., Levin, R. D., Burgess Jr., D. R., Orkin, V. L., Tsang, W., McGivern, W. S., Hudgens, J. W., Knyazev, V. D., Atkinson, D. B., Cahi, E., Tereza, A. M., Lin, C.-Y., Allison, T. C., Mallard, W. G., Westley, F., Herron, J. T., Hampson, R. F., and Frizzell, D. H.: http://kinetics.nist.gov/, 2015.

Marx, O., Brummer, C., Ammann, C., Wolff, V., and Freibauer, A.: TRANC – a novel fast-response converter to measure total reactive atmospheric nitrogen, Atmos. Meas. Tech., 5, 1045-1057, 2012.

May, A. A., McMeeking, G. R., Lee, T., Taylor, J. W., Craven, J. S., Burling, I. R., Sullivan, A. P., Akagi, S. K., Collett, J. L. J., Flynn, M., Coe, H., Urbanski, S. P., Seinfeld, J. H., Yokelson, R. J., and Kreidenweis, S. M.: Aerosol emissions from prescribed fires in the United States: A synthesis of laboratory and aircraft measurements, J. Geophys. Res., 119, 2014.

McMeeking, G. R., Kreidenweis, S. M., Baker, S., Carrico, C. M., Chow, J. C., Collett Jr., J. L., Hao, W. M., Holden, A. S., Kirchstetter, T. W., Malm, W. C., Moosmuller, H., Sullivan, A. P., and Wold, C. E.: Emissions of trace gases and aerosols during the open combustion of biomass in the laboratory, J. Geophys. Res., 114, doi:10.1029/2009JD011836, 2009.

Min, K. E., Washenfelder, R. A., Dube, W. P., Langford, A. O., Edwards, P. M., Zarzana, K. J., Stutz, J., Lu, K., Rohrer, F., Zhang, Y., and Brown, S. S.: A broadband cavity enhanced absorption spectrometer for aircraft measurements of glyoxal, methylglyoxal, nitrous acid, nitrogen dioxide, and water vapor, Atmos. Meas. Tech., 9, 423-440., 2016.

NOAA: https://www.esrl.noaa.gov/csd/projects/firex/2018.

Paatero, P. and Tapper, U.: Positive matrix factorization: A non-negative factor model with optimal utilization of error estimates of data values. , Environmetrics, 5, 111-126, 1994.

Prenni, A. J., Levin, E. J. T., Benedict, K. B., Sullivan, A. P., Schurman, M. I., Gebhart, K. A., Day, D. E., Carrico, C. M., Malm, W. C., Schichtel, B. A., Collett Jr., J. L., and Kreidenweis, S. M.: Gas-phase reactive nitrogen near Grand Teton National Park: Impacts of transport, anthropogenic emissions, and biomass burning, Atmos Environ., 89, 749-756, 2014.

Ren, Q. Q., Zhao, C. S., Wu, X. X., Liang, C., Chen, X. P., Shen, J. Z., and Wang, Z.: Formation of $NO_x$ precursors during wheat straw pyrolysis and gasification with $O_2$ and $CO_2$, Fuel, 89, 1064-1069, 2010.

762 Roberts, J. M., Langford, A. O., Goldan, P. D., and Fehsenfeld, F. C.: Ammonia measurements at Niwot
763 Ridge, Colorado, and Point Arena, California, using the tungsten oxide denuder tube technique, J. Atmos.
764 Chem., 7, 137-152, 1988.
765
766 Roberts, J. M., Veres, P. R., Cochran, A. K., Warneke, C., Burling, I. R., Yokelson, R. J., Lerner, B. M.,
767 Gilman, J. B., Kuster, W. C., Fall, R., and de Gouw, J.: Isocyanic acid in the atmosphere and its possible
768 link to smoke-related health effects, PNAS, 108, 8966-8971, 2011.
769
770 Saylor, R. D., Edgerton, E. S., Hartsell, B. E., Baumann, K., and Hansen, D. A.: Continuous gaseous and
771 total ammonia measurements from the southeastern aerosol research and characterization (SEARCH)
772 study, Atmos. Environ., 44, 4994-5004, 2010.
773
774 Schwab, J. J., Li, Y., Bae, M.-S., Demerjian, K. L., Hou, J., Zhou, X., Jensen, B., and Pryor, S.: A
775 laboratory intercomparision of real-time gaseous ammonia measurement methods, Environ. Sci. Technol.,
776 41, 8412-8419, 2007.
777
778 Sekimoto, K., Li, S.-M., Yuan, B., Koss, A. R., Coggon, M. M., Warneke, C., and de Gouw, J.:
779 Calculation of the sensitivity of proton-transfer-reaction mass spectrometry (PTR-MS) for organic trace
780 gases using molecular properties, Int. J. Mass Spectrom., 421, 71-94, 2017.
781
782 Sekimoto, K., Koss, A. R., Gilman, J. B., Selimovic, V., Coggon, M. M., Zarzana, K. J., Yuan, B.,
783 Lerner, B. M., Brown, S. S., Warneke, C., Yokelson, R. J., Roberts, J. M., and de Gouw, J.: High- and
784 low-temperature pyrolysis profiles describe primary emissions of volatile organic compounds from
785 western US wildfire fuels, Atmos. Chem. Phys., 18, 9263-9281, 2018.
786
787 Selimovic, V., Yokelson, R. J., Warneke, C., Roberts, J. M., deGouw, J. A., Reardon, J., and Griffith, D.
788 W. T.: Aerosol optical properties and trace gas emissions by PAX and OP-FTIR for laboratory-simulated
789 western US wildfires during FIREX, Atmos. Chem. Phys., 18, 2929-2948, 2018.
790
791 Shaddix, C. R., Harrington, J. E., and Smyth, K. C.: Quantitative measurements of enhanced soot
792 production in a flickering methane/air diffusion flame, Combust. Flame, 99, 723-732, 1994.
793
794 Stockwell, C. E., Christian, T. J., Goetz, J. D., Jayarathne, T., Bhave, P. V., Praveen, P. S., Adhikari, S.,
795 Maharjan, R., DeCarlo, P. F., Stone, E. A., Saikawa, E., Blake, D. R., Simpson, I. J., Yokelson, R. J., and
796 Panday, A. K.: Nepal Ambient Monitoring and Source Testing Experiment (NAMaSTE): emissions of
797 trace gases and light-absorbing carbon from wood and dung cooking fires, garbage and crop residue
798 burning, brick kilns, and other sources, Atmos. Chem. Phys., 16, 11043-11081, 2016a.
799
800 Stockwell, C. E., Jayarathne, T., Cochrane, M. A., Ryan, K. C., Putra, E. I., Saharjo, B. H., Nurhayati, A.
801 D., Albar, I., Blake, D. R., Simpson, I. J., Stone, E. A., and Yokelson, R. J.: Field measurements of trace
802 gases and aerosols emitted by peat fires in Central Kalimantan, Indonesia, during the 2015 El Niño,
803 Atmos. Chem. Phys., 16, 11711 - 11732, 2016b.
804
805 Stockwell, C. E., Kupc, A., Witkowski, B., Talukdar, R. K., Liu, Y., Selimovic, V., Zarzana, K. J.,
806 Sekimoto, K., Warneke, C., Washenfelder, R. A., Yokelson, R. J., Middlebrook, A. M., and Roberts, J.
807 M.: Characterization of a catalyst-based conversion technique to measure total particle nitrogen and
808 organic carbon and comparison to a particle mass measurement instrument, Atmos. Meas. Tech., 11,
809 2749-2768, 2018.
810

811 Stockwell, C. E., Veres, P. R., Williams, J., and Yokelson, R. J.: Characterization of biomass burning
812 smoke from cooking fires, peat, crop residue and other fuels with high resolution proton-transfer-reaction
813 time-of-flight mass spectrometry, Atmos. Chem. Phys. , 15, 845-865, 2015.
814
815 Stockwell, C. E., Yokelson, R. J., Kreidenweis, S. M., Robinson, A. L., DeMott, P. J., Sullivan, R. C.,
816 Reardon, J., Ryan, K. C., Griffith, D. W. T., and Stevens, L.: Trace gas emissions from combustion of
817 peat, crop residue, domestic biofuels, grasses, and other fuels: configuration and Fourier transform
818 infrared (FTIR) component of the fourth Fire Lab at Missoula Experiment (FLAME-4),, Atmos. Chem.
819 Phys., 14, 9727-9754, 2014.
820
821 Taylor, S. W., Wotton, B. M., Alexander, M. E., and Dalrymple, G. N.: Variation in wind and crown fire
822 behaviour in a northern jack pine–black spruceforest., Canadian J. Forest Res., 34, 1561-1576, 2004.
823
824 Ulbrich, I. M., Canagaratna, M. R., Zhang, Q., Worsnop, D. R., and Jimenez, J. L.: Interpretation of
825 organic components form Postive Matrix Factorization of aerosol mass spectrometric data, Atmos. Chem.
826 Phys., 9, 2891-2918, 2009.
827
828 Veres, P. R., Roberts, J. M., Burling, I. R., Warneke, C., de Gouw, J., and Yokelson, R. J.: Measurements
829 of gas-phase inorganic and organic acids from biomass fires by negative-ion proton-transfer chemical-
830 ionization mass spectrometry (NI-PT-CIMS), J. Geophys. Res.-Atmos., 115, D23302, 2010.
831
832 Warneke, C., Roberts, J. M., Veres, P., Gilman, J. B., Kuster, W. C., Burling, I. R., Yokelson, R. J., and
833 de Gouw, J. A.: VOC identification and inter-comparison from laboratory biomass burning using PTR-
834 MS and PIT-MS, Int. J. Mass Spectrom., 303, 6-14, 2011.
835
836 Westerling, A. L., Hidalgo, H. G., Cayan, D. R., and Swetnam, T. W.: Warming and Earlier Spring
837 Increase Western U.S. Forest Wildfire Activity, Science, 313, 940-943, 2006.
838
839 Williams, E. J., Baumann, K., Roberts, J. M., Bertman, S. B., Norton, R. B., Fehsenfeld, F. C.,
840 Springston, S. R., Nunnermacker, L. J., Newman, L., Olszyna, K., Meagher, J., Hartsell, B., Edgerton, E.,
841 Pearson, J. R., and Rodgers, M. O.: Intercomparison of ground-based $NO_y$ measurement techniques, J.
842 Geophys. Res.-Atmospheres, 103, 22261-22280, doi: 22210.21029/22298JD00074, 1998.
843
844 Wotton, B. M., Gould, J. S., McCaw, W. L., Cheney, N. P., and Taylor, S. W.: Flame temperature and
845 residence time of fires in dry eucalypt forest, Int. J. Wildland Fire, 21, 270-281, 2012.
846
847 Yokelson, R. J., Andreae, M. O., and Akagi, S. K.: Pitfalls with the use of enhancement ratios or
848 normalized excess mixing ratios measured in plumes to characterize pollution sources and aging, Atmos.
849 Meas. Tech., 6, 2155-2158, 2013a.
850
851 Yokelson, R. J., Burling, I. R., Gilman, J. B., Warneke, C., Stockwell, C. E., de Gouw, J. A., Akagi, S. K.,
852 Urbanski, S. P., Veres, P., Roberts, J. M., Kuster, W. C., Reardon, J., Griffith, D. W. T., Johnson, T. J.,
853 Hosseini, S., Miller, J. W., Cocker III, D. R., Jung, H., and Weise, D. R.: Coupling field and laboratory
854 measurements to estimate the emission factors of identified and unidentified trace gases for prescribed
855 fires, Atmos. Chem. Phys., 13, 89-116, 2013b.
856
857 Yokelson, R. J., Crounse, J. D., DeCarlo, P. F., Karl, T., Urbanski, S., Atlas, E., Campos, T., Shinozuka,
858 Y., Kapustin, V., Clarke, A. D., Weinheimer, A. J., Knapp, D. J., Montzka, D. D., Holloway, J.,
859 Weibring, P., Flocke, F. M., Zheng, W., Toohey, D., Wennberg, P. O., Wiedinmyer, C., Mauldin, L.,
860 Fried, A., Richter, D., Walega, J., Jimenez, J. L., Adachi, K., Buseck, P. R., Hall, S. R., and Shetter, R. E.:
861 Emissions from biomass burning in the Yucatan, Atmos. Chem. Phys., 9, 5785-5812, 2009.

Zarzana, K. J., Selimovic, V., Koss, A. R., Sekimoto, K., Coggon, M. M., Yuan, B., Dube, W. P., Yokelson, R. J., Warneke, C., de Gouw, J. A., Roberts, J. M., and Brown, S. S.: Primary emissions of glyoxal and methylglyoxal from laboratory measurements of open biomass burning, Atmos. Chem. Phys., 18, 15451-15470, 2018.

**Table 1. Nitrogen compounds observed in the FIREX FireLab 2016 Study.**

| Compound/Class | Importance | Measurement Method | Method Reference |
|---|---|---|---|
| Total Reactive N | Total available for atmospheric reactions | Catalytic Conversion $NO/O_3$ chemiluminescence | Stockwell et al., 2018 |
| Nitric Oxide | Major "flaming stage" product, oxidant production | $NO/O_3$ chemiluminescence OP-FTIR (Open Path Fourier Transform Infrared) | Williams et al., 1998 Selimovic et al., 2018 |
| Nitrogen Dioxide | Atmospheric oxidant production | OP-FTIR, ACES (Airborne Cavity-Enhanced Spectometer) | Stockwell et al., 2014, Min et al., 2016, Zarzana, et al., 2018 |
| Nitrous Acid | $HO_x$ radical source | OP-FTIR, ACES | Stockwell et al., 2014, Min et al., 2016, Zarzana et al., 2018 |
| Nitric Acid[1] | Particle precursor | OP-FTIR | Yokelson et al 2009, McMeeking et al 2009 |
| Hydrogen Cyanide | Flame chemistry, Atmospheric tracer, Toxicity | OP-FTIR, PTR-ToF-MS (Proton Transfer Reaction Time of Flight Mass Spectrometer) | Selimovic, et al., 2018 Koss, et al., 2018 |
| Isocyanic Acid | Flame chemistry, Toxicity, Health effects | PTR-ToF-MS | Koss, et al., 2018 |
| Ammonia | Major "smoldering stage" product, Main atmospheric base, Particle formation | OP-FTIR | Selimovic, et al., 2018 |
| NVOCs:<br>Amides[2]<br>Amines[3]<br>Heterocyclics[4]<br>Nitriles[5]<br>Nitro compds[6] | Brown carbon, Toxicity, Tracers | PTR-ToF-MS, GC/MS (Gas Chromatography Mass Spectrometry), $I^-$ CIMS (Iodide ion Chemical Ionization Mass Spectrometer. | Koss, et al., 2018 Gilman et al., 2015 Lerner et al., 2017 Lee et al., 2014 |

1). The OP-FTIR has a 10ppbv detection for gas phase $HNO_3$, but $HNO_3$ was not observed above detection limit.
2). Ethylamine, methanimine, propeneamine, sulfinylmethanamine, trimethylamine, buteneamines
3). Formamide, acetamide, methylmaleimide
4). $C_2$-pyrroles, dihydropyridine, ethynylpyrrole, methylpyridine, methylpyrrole, pyridinealdehyde, 4-pyrindinol, vinylpyridine
5). Acetonitrile, acrylonitrile, benzonitrile, butanenitrile, butynenitrile, benzoacetonitrile, $C_7$acrylonitrile, $C_8$-nitriles, heptylnitrile, furancarbonitrile, methylbenzoacetonitrile, pentylnitriles, propanenitrile, propynenitrile, butenenitrile, methylisocyanate.
6). Butenenitrates, nitrobenzene, nitroethane, nitroethene, nitrofuran, nitromethane, nitropropanes, nitrotoluene.

**Table 2. Compounds and compound classes used in the PMF analyses and their corresponding errors.**

| Compound or Class | unit | Estimated error |
|---|---|---|
| $NH_3$ | ppbv | 5% + 2 ppbv |
| NO | ppbv | 10% + 1 ppbv |
| $NO_2$ | ppbv | 10% + 0.2 ppbv |
| HONO | ppbv | 20% + 1 ppbv |
| HCN | ppbv | 15% + 0.2 ppbv |
| HNCO | ppbv | 15% + 0.2 ppbv |
| Nitriles | ppbv | 20% + 0.2 ppbv |
| Amines | ppbv | 20% + 0.2 ppbv |
| Amides | ppbv | 20% + 0.2 ppbv |
| Nitro-compounds | ppbv | 20% + 0.2 ppbv |
| Heterocyclics | ppbv | 20% + 0.2 ppbv |

**Table 3. Summary of $X_i/N_r$ Measurements for all Stack Burns[1]**

| **Quantity** | **Average ±(std dev) %** |
|---|---|
| $NO/N_r$ | 34.5 (16.6) |
| $NO_2/N_r$ | 9.4 (6.2) |
| $HNCO/N_r$ | 6.0 (2.9) |
| $HONO/N_r$ | 4.5 (2.2) |
| $HCN/N_r$ | 4.3 (2.3) |
| $NH_3/N_r$ | 19.3 (6.7) |
| $NVOC/N_r$ | 4.3 (2.8) |
| $(N_r\text{-sumN})/N_r$ | 15.2 (9.8) |

1). Not every measurement was available for every fire, consequently the values do not add up to exactly 100%.

**Table 4. Residuals of the PMF analyses by fuel, as percent of total signal**

| Fuel | Total Number | Component | Fire Number | Residual (%), avg (stdev) |
|---|---|---|---|---|
| Ponderosa Pine | 9 | Realistic (mix) | Fire 37,59,72 | 3.8 (± 1.4) |
| | | Canopy (pure) | Fire 19[a],39 | |
| | | Litter (pure) | Fire 38 | |
| Lodgepole Pine | 5 | Realistic | Fire 07[a],58,63 | 5.1 (±3.1) |
| | | Canopy | Fire 40 | |
| | | Litter | Fire 41 | |
| Douglas Fir | 4 | Realistic | Fire 14[a],57 | 6.8 (±3.1) |
| | | Canopy | Fire 18 | |
| | | Litter | Fire 43[a] | |
| SubAlpine Fir | 5 | Realistic | Fire 47,67 | 6.6 (±2.3) |
| | | Canopy | Fire 15,23 | |
| | | Litter | Fire 51[a] | |
| Engelmann Spruce | 2 | Realistic | Fire 08[a] | 3.1 (±1.9) |
| | | Canopy | Fire 25 | |
| Chamise (San Dimas, CA) | 2 | Canopy | Fire 24,29 | 4.4 (±2.7) |
| Chamise (North Mountain, CA.) | 2 | Canopy | Fire 27,32 | 4.2 (±1.0) |
| Manzanita San Dimas, CA) | 2 | Canopy | Fire 30,33 | 4.8 (±2.1) |
| Manzanita (North Mountain, CA.)) | 2 | Canopy | Fire 28 | 5.1 |

a-Excluded from Batch 2

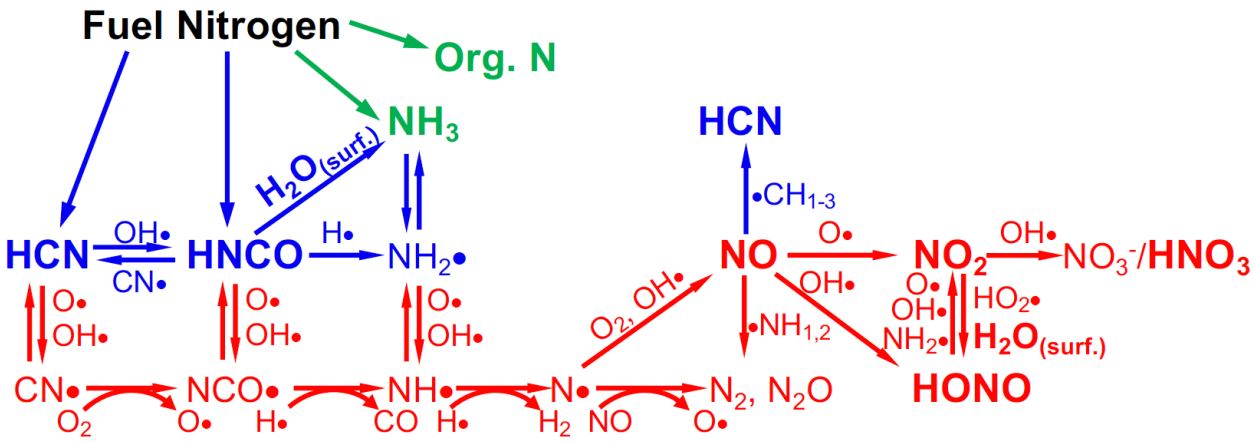


**Figure 1. Schematic of the combustion chemistry of the small molecules that are emitted from BB and represent sources and sinks of reactive nitrogen ($N_r$), adapted from (Glarborg et al., 2018; Lobert and Warnatz, 1993; Lucassen et al., 2012; Manion et al., 2015). $H_2O_{(surf)}$ denotes the combination of $H_2O$ and a surface to facilitate the reaction. Red color indicates the highest temperature (combustion) processes, blue indicates intermediate temperature processes and green indicates the lowest temperature processes. The species that are measured in this work are shown in bold and slightly larger text.**

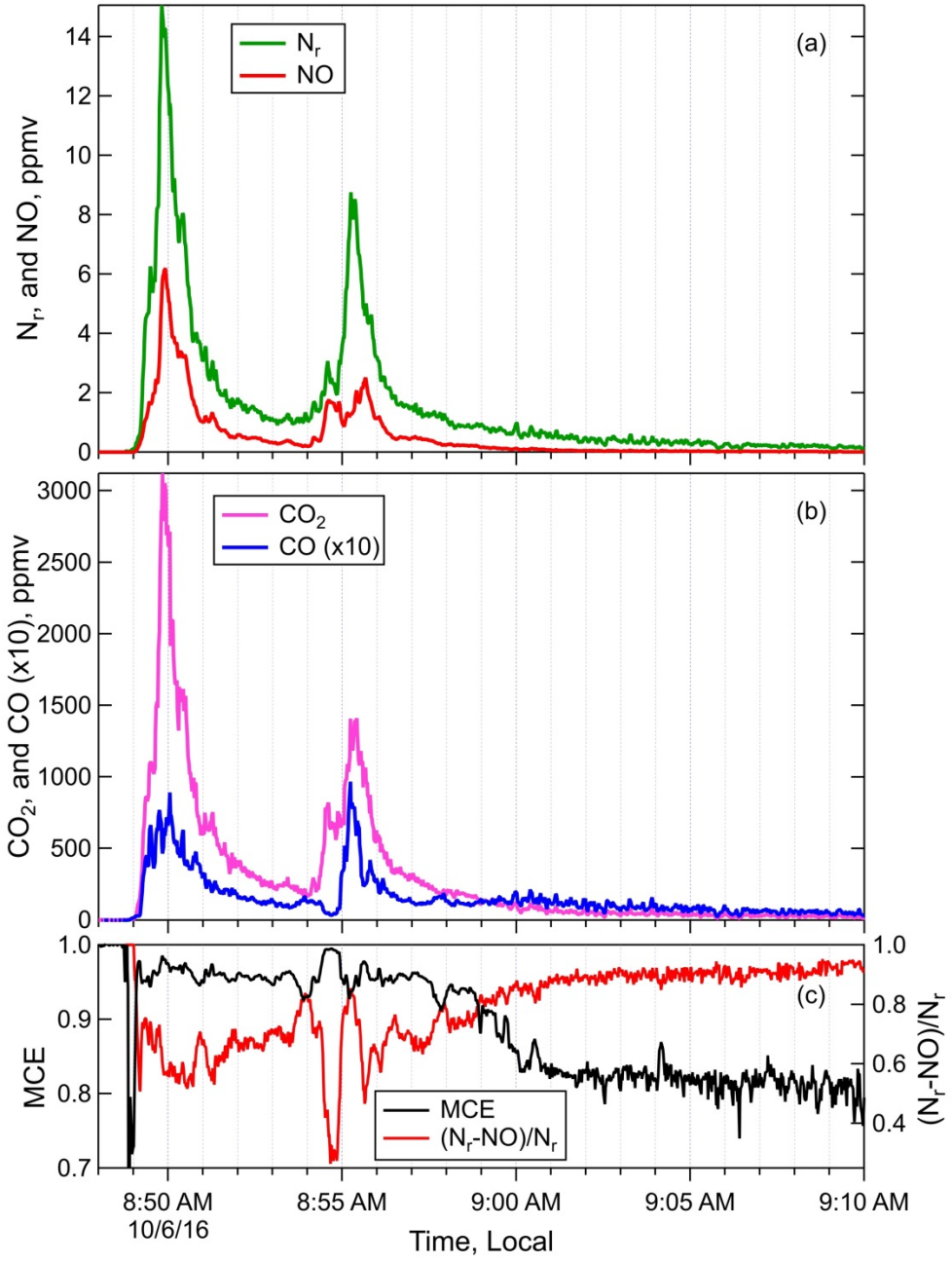


**Figure 2. Timelines of the $N_r$, NO (panel a), $\Delta CO_2$, $\Delta CO$ (panel b), MCE and $(N_r\text{-NO})/N_r$ (panel c) measured during Fire 004, a ponderosa pine realistic mix sample. Note that $\Delta CO$ is plotted at x10 the measured abundance for clarity.**

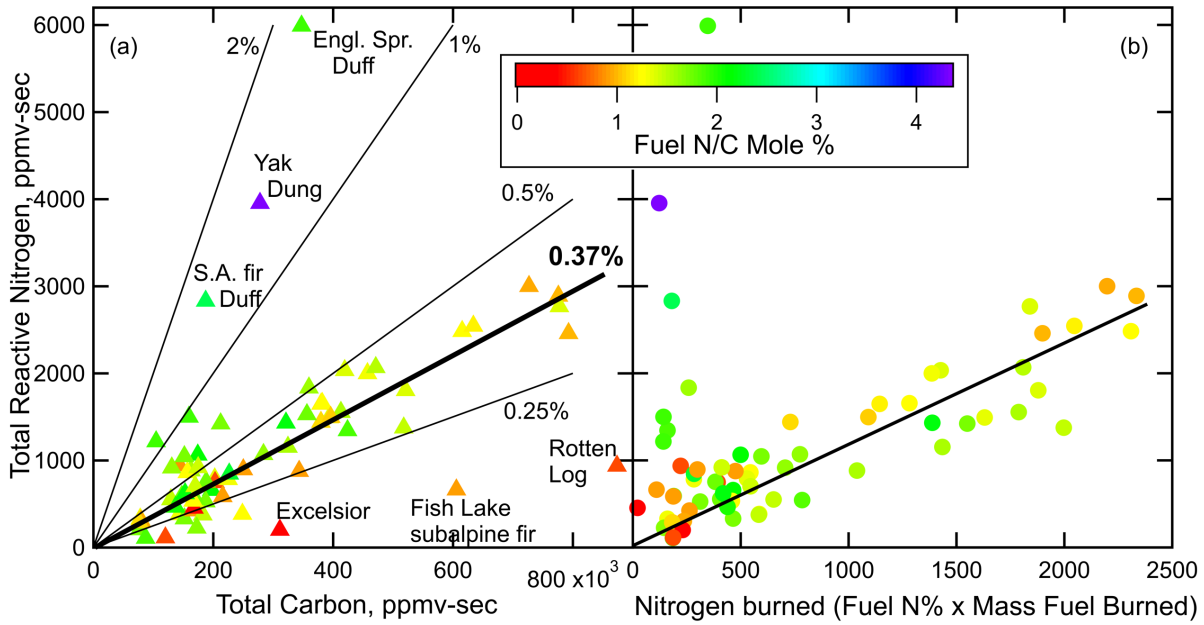


**Figure 3. Integrated $N_r$ versus integrated Total Carbon (panel a), and versus nitrogen burned based on fuel nitrogen content and mass of fuel burned (panel b). The points are colored by fuel nitrogen to carbon ratio. Note that the x and y scales on panel (a) are different by more than a factor of 100.**

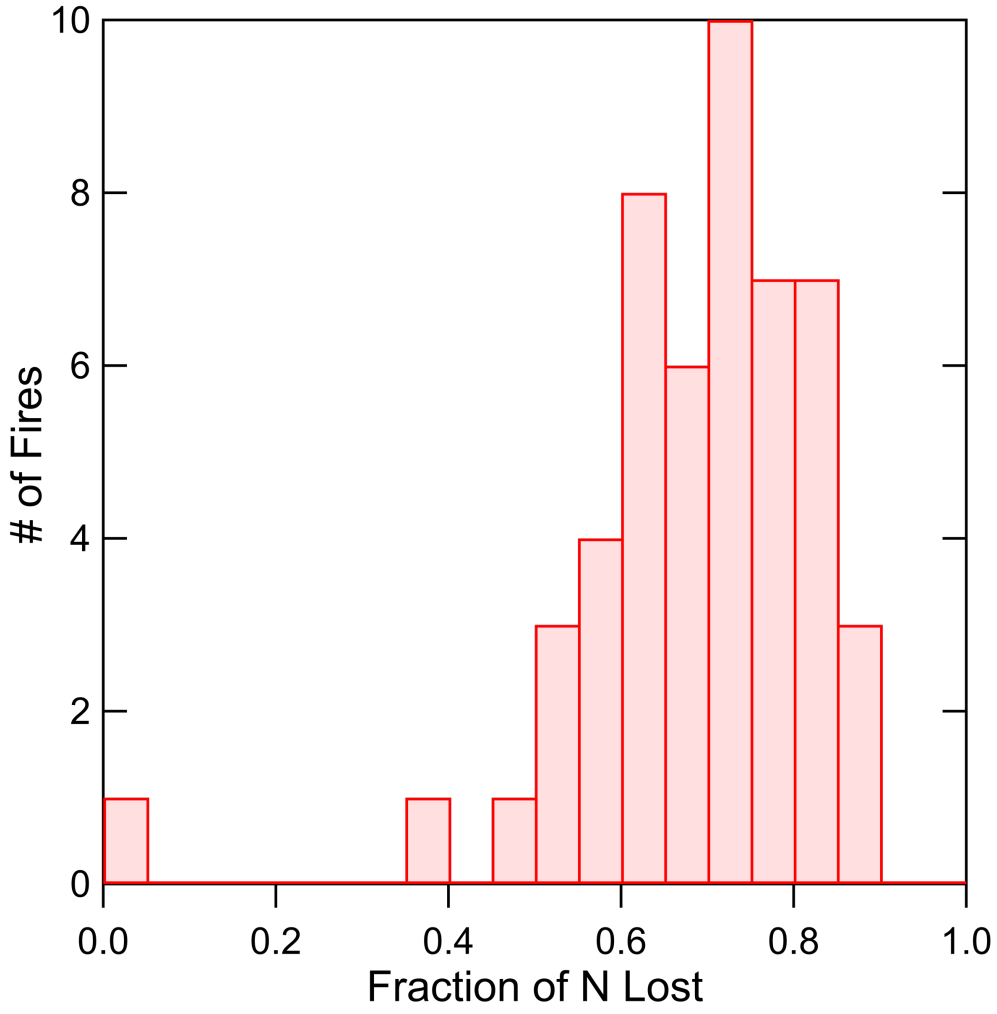


**Figure 4. The histogram of the fraction of N loss to $N_2$ and $N_2O$ estimated from the mass balance analysis described in the Supplemental Materials (52 burns).**

935

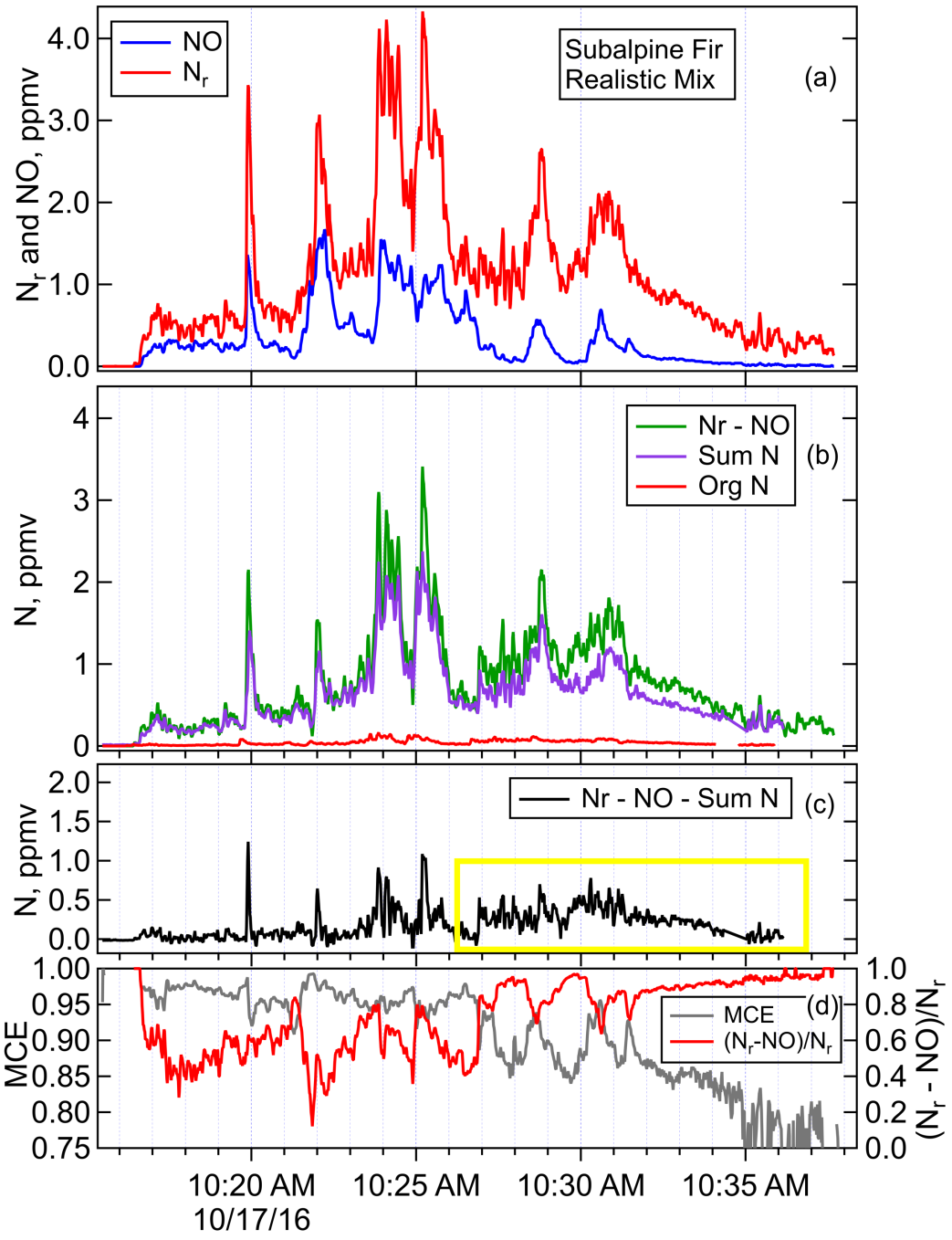


936
937 **Figure 5. Timelines of $N_r$ and NO (panel a), $N_r$ – NO, the sum of all measures N species except**
938 **for NO (panel b), residual of $N_r$ minus all measured N species ($N_r$ – NO – Sum N, panel c),**
939 **and MCE and ($N_r$ – NO)/$N_r$ (panel d) for Fire047, subalpine fir realistic mix. The yellow box**
940 **highlights the area of higher residual $N_r$ that corresponds to more smoldering emissions.**
941
942

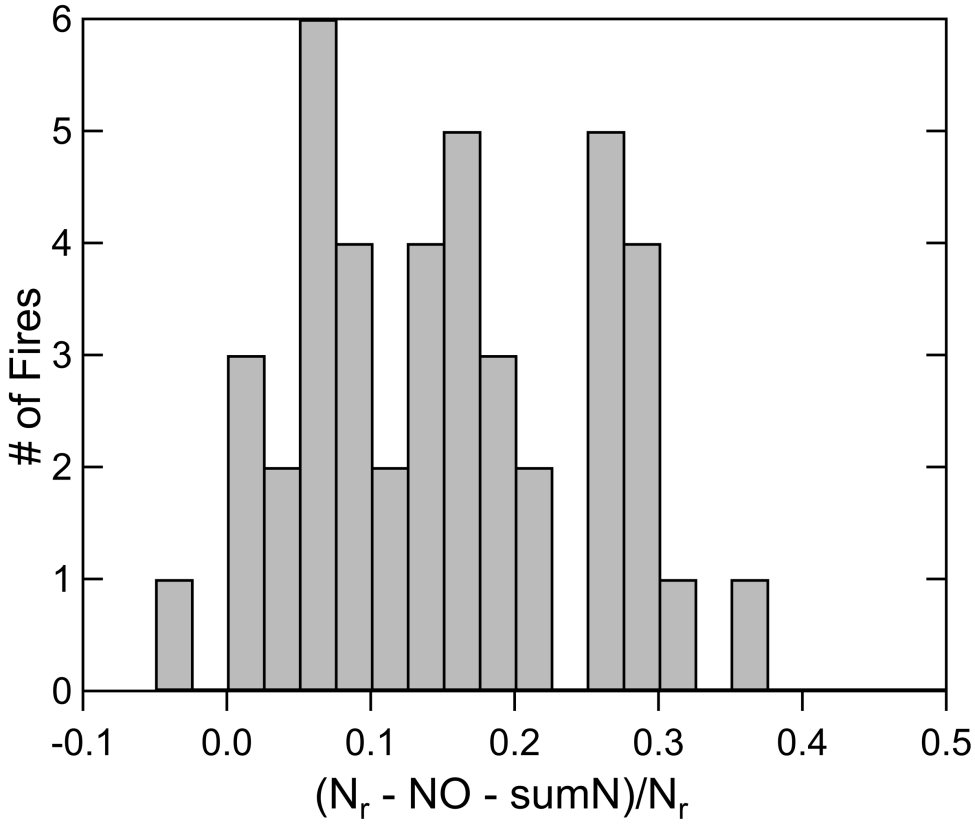


**Figure 6. A histogram of the residual N for all the stack fires during the 2016 FireLab study for which there are FTIR, ACES and PTR-ToF measurements (n=43). The median is 0.143, and the mean (±std dev) was 0.15 (±0.10).**

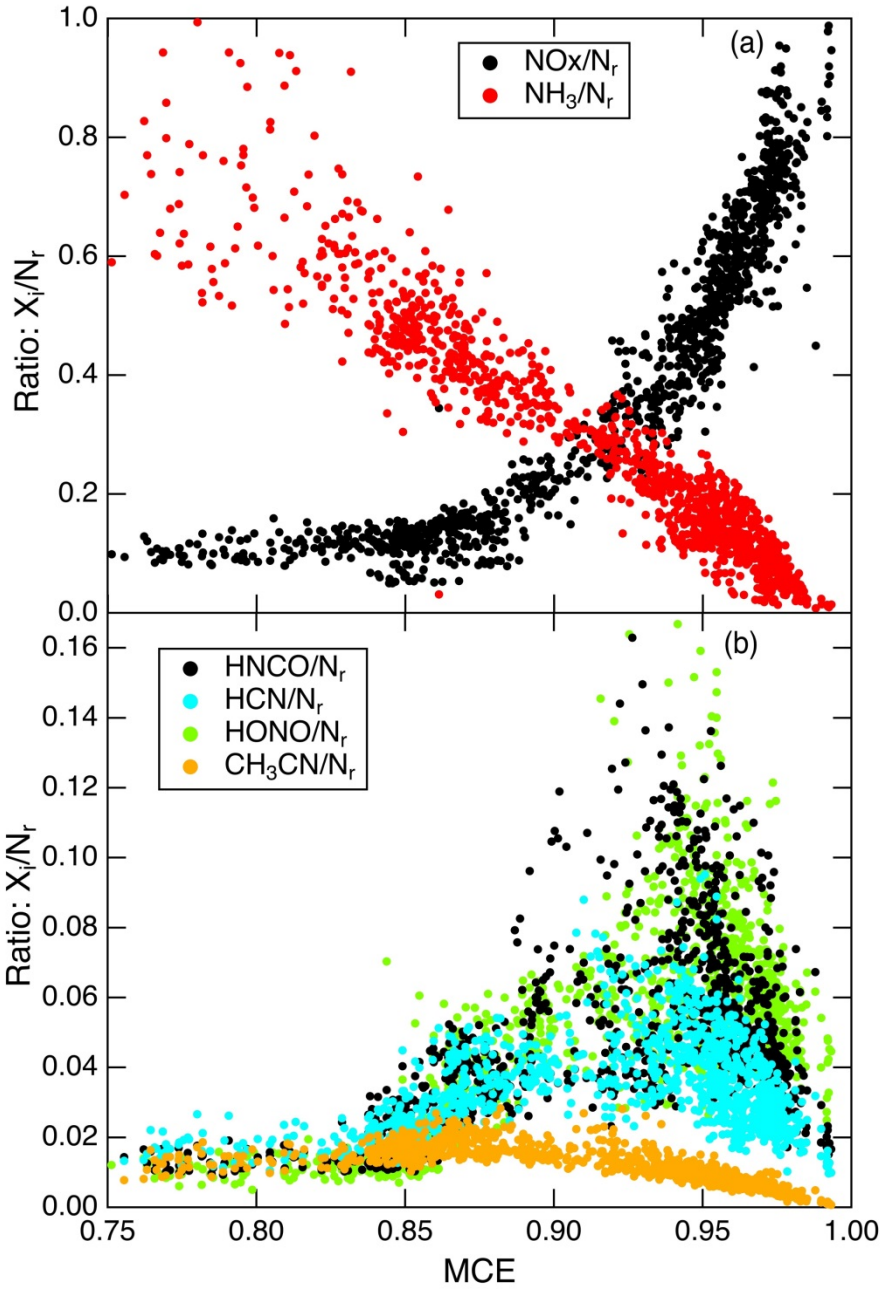


**Figure 7. The relationships between $NO_x/N_r$ and $NH_3/N_r$ vs MCE (panel a), and the $HNCO/N_r$, $HCN/N_r$, $HONO/N_r$, and $CH_3CN/N_r$ vs MCE (panel b) for Fire 047.**

962

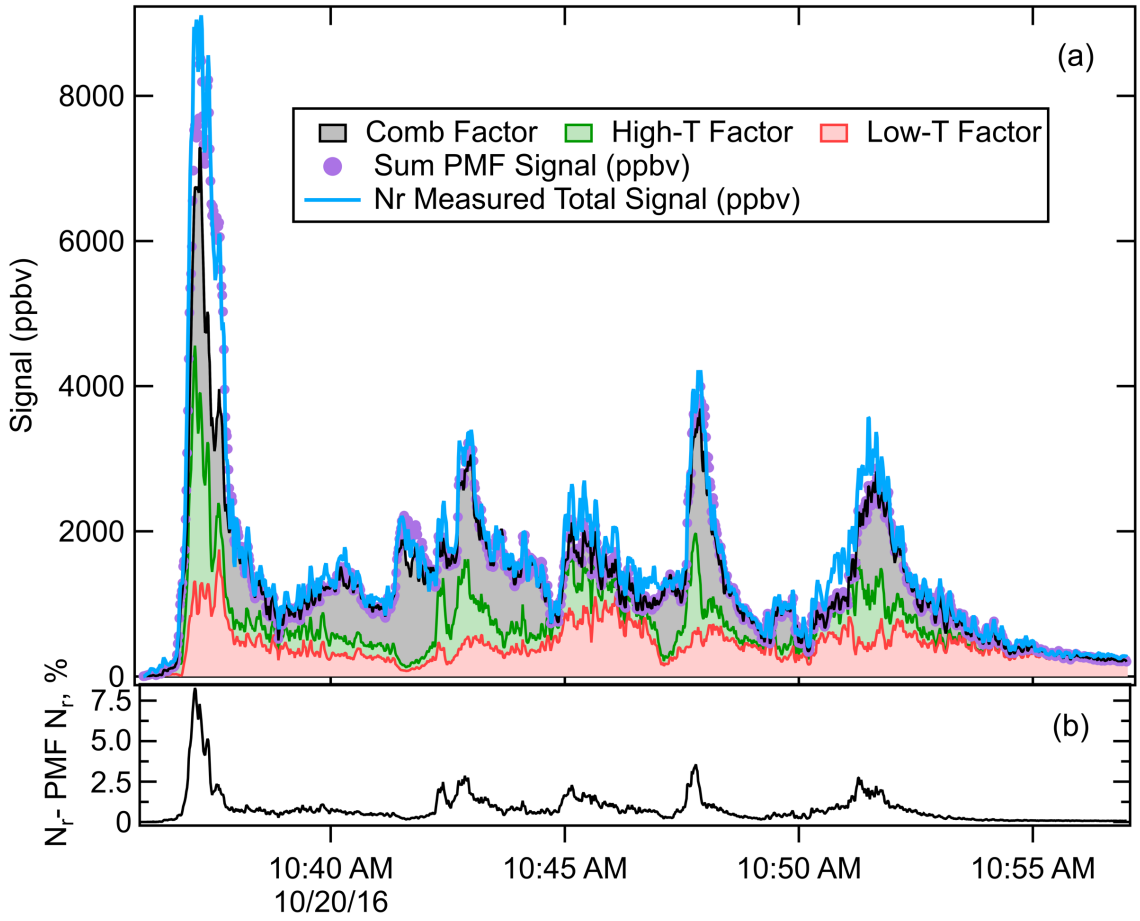


963

964 **Figure 8. Pane (a), the measured $N_r$ signal for Fire 063 (lodgepole pine) (blue line), the sum**
965 **of the signal reconstructed by the PMF (purple points) and the three PMF factors:**
966 **combustion (grey), high temperature (green) and low temperature (red), plotted in a stacked**
967 **fashion (i.e. added on top of one another). Panel (b) the "residual" of the PMF fit consisting**
968 **of the measured $N_r$ signal minus the $N_r$ signal reconstructed by the PMF, as a percentage of**
969 **the $N_r$ signal.**

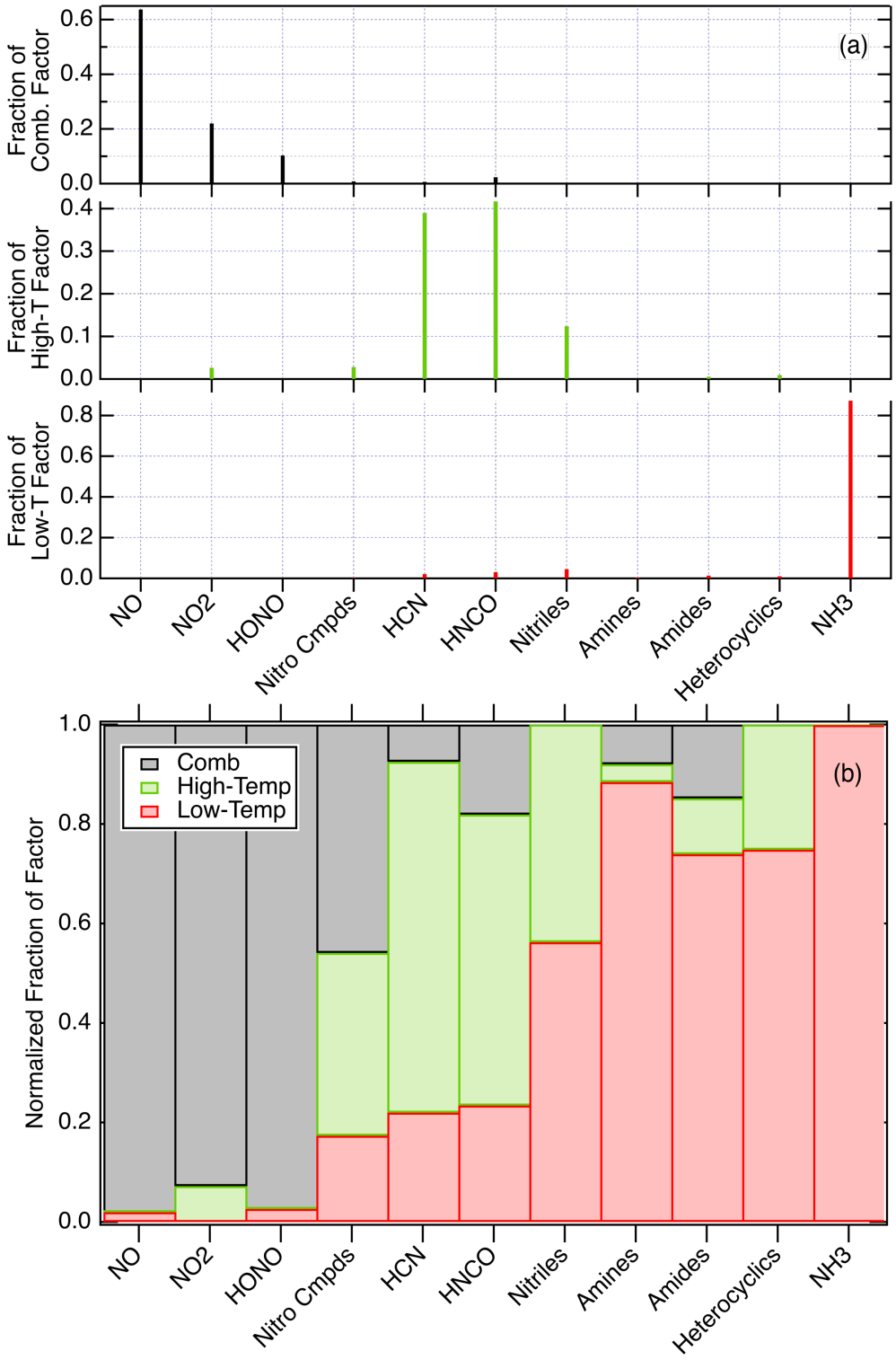


**Figure 9. The contributions of nitrogen species to the factors that simulate the emissions from coniferous fuels shown in Figure S2 (panel a), and the fraction of each compound or class found in each factor (panel b).**

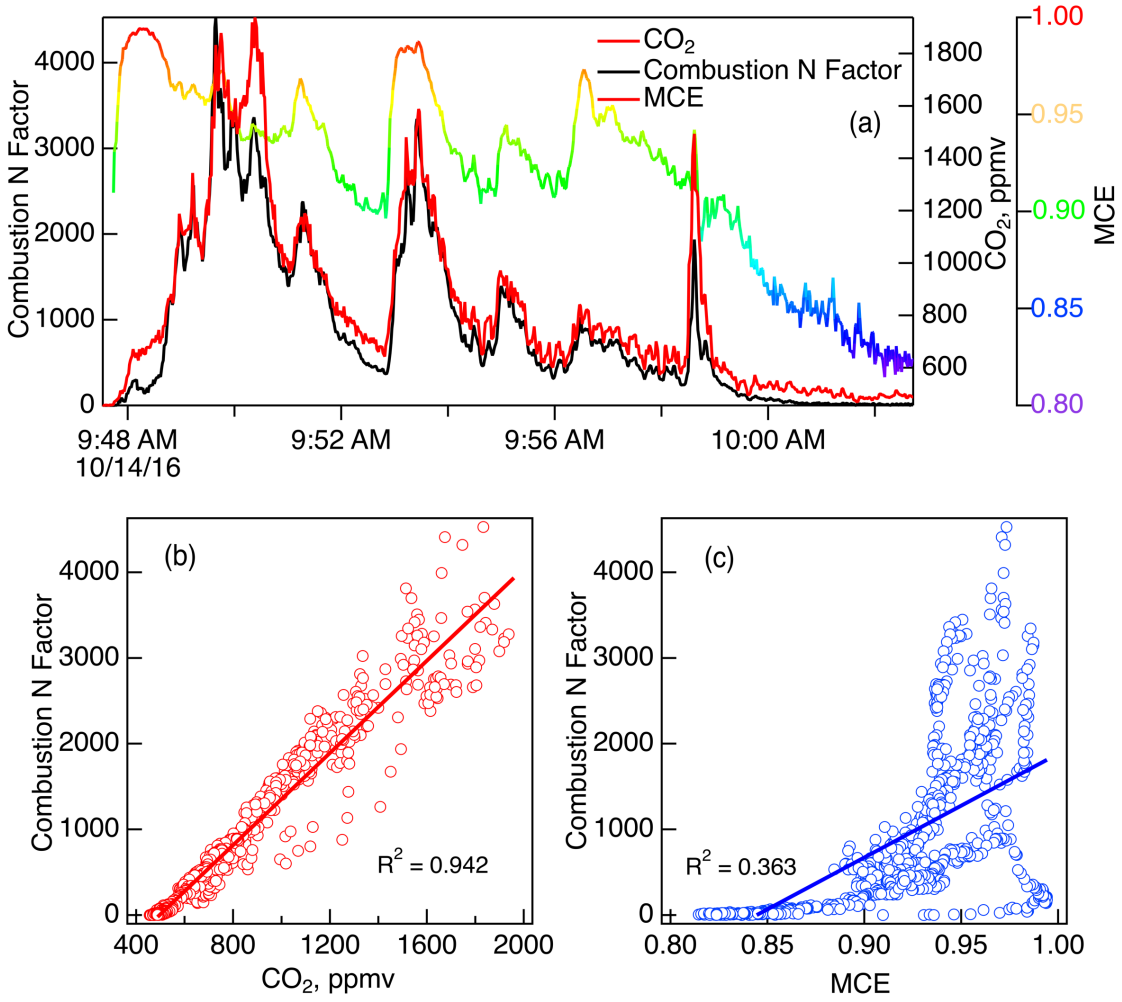


974
975 **Figure 10. Comparisons of the N-PMF combustion factor (Comb-N) with $CO_2$ and MCE**
976 **(Panel a) for Fire 037 (ponderosa pine). Panel (b) shows the scatter plot of the Comb-N**
977 **factor versus $CO_2$ and panel (c) shows the scatter plot of Comb-N factor versus MCE.**

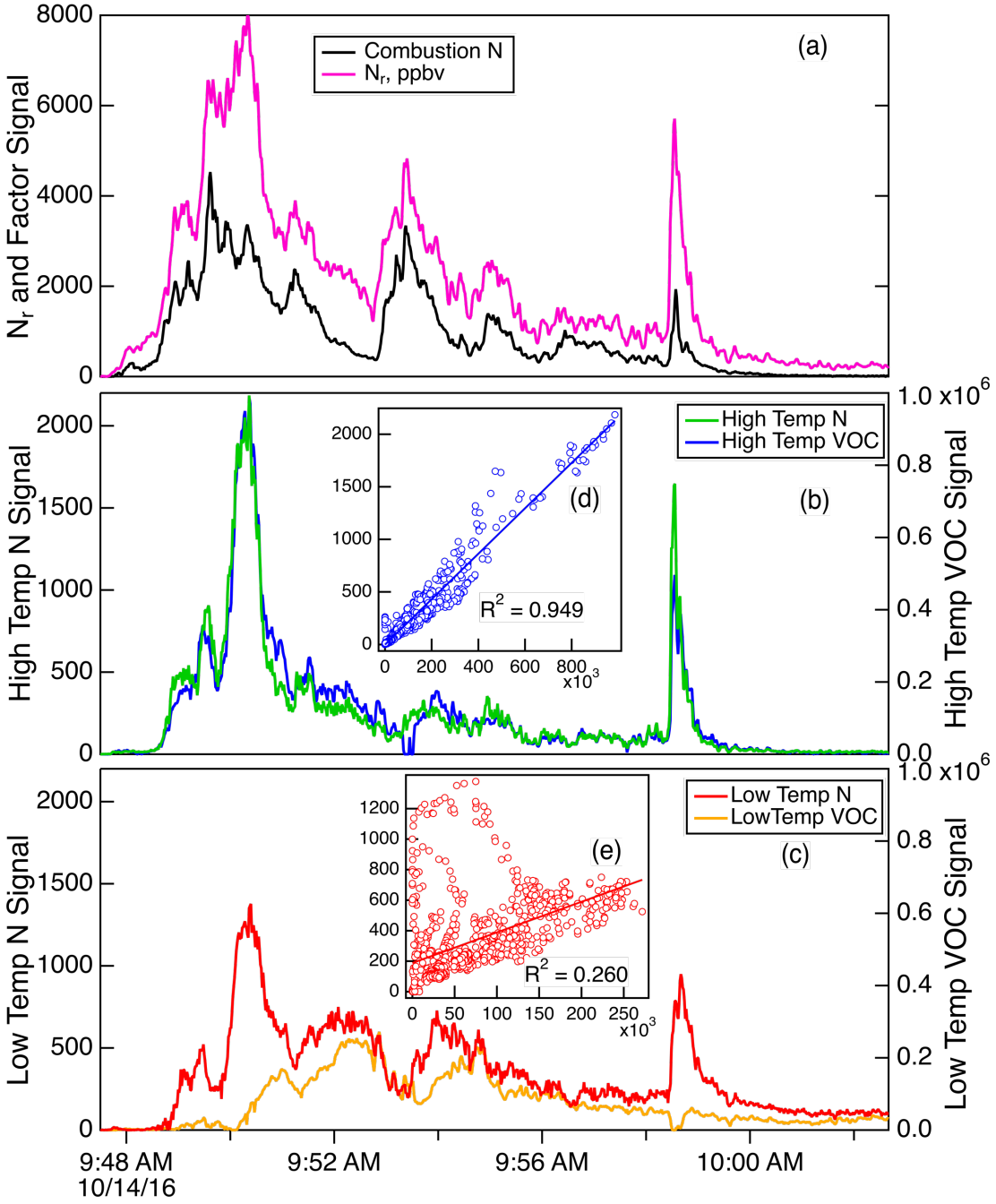


978
979 **Figure 11. Details of the PMF factors for Fire 037 (ponderosa pine). Panel (a) shows the total**
980 **$N_r$ signal (magenta) and the Comb-N factor (black), panel (b) shows the HT-N factor (green)**
981 **and HT- VOC factor (blue), and panel (c) shows the LT-N factor (red) and LT-VOC factor**
982 **(orange). The insets (panel d) show the correlation of the two HT factors and the correlation**
983 **between the two LT factors.**
984
985
986